UNIVERSITÄTSKLINIKUM HAMBURG-EPPENDORF

Bernhard-Nocht-Institut für Tropenmedizin
Abteilung Immunologie
Prof. Dr. med. Bernhard Fleischer

Beeinträchtigung der Monozytenantwort bei CCR2-Defizienz im Mausmodell während der Infektion mit *Orientia tsutsugamushi*

Dissertation

zur Erlangung des Grades eines Doktors der Medizin
an der Medizinischen Fakultät der Universität Hamburg

vorgelegt von:

Karl Michael Petermann
aus Hamburg
geboren in Henstedt-Ulzburg

Hamburg 2022

Angenommen von der
Medizinischen Fakultät der Universität Hamburg am: 22.11.2022

Veröffentlicht mit Genehmigung der
Medizinischen Fakultät der Universität Hamburg.

Prüfungsausschuss, der/die Vorsitzende: **Prof. Dr. Friedrich Haag**

Prüfungsausschuss, zweite/r Gutachter/in: **Prof. Dr. Bernhard Fleischer**

Inhaltsverzeichnis

1. Publizierter Artikel

Front Immunol. 2021; 12: 670219. Published online 2021 Jul 5.

doi: 10.3389/fimmu.2021.670219

frontiers in Immunology

ORIGINAL RESEARCH
published: 05 July 2021
doi: 10.3389/fimmu.2021.670219

Check for updates

CCR2 Deficiency Impairs Ly6C^{lo} and Ly6C^{hi} Monocyte Responses in *Orientia tsutsugamushi* Infection

*Michael Petermann[1], Zacharias Orfanos[2], Julie Sellau[1], Mohammad Gharaibeh[1,3], Hannelore Lotter[1], Bernhard Fleischer[1] and Christian Keller[1,2]**

[1] Department of Molecular Biology and Immunology, Bernhard Nocht Institute for Tropical Medicine, Hamburg, Germany, [2] Institute of Virology, University Hospital Giessen and Marburg, Marburg, Germany, [3] Department of Basic Veterinary Medical Science, Jordan University of Science and Technology, Faculty of Veterinary Medicine, Irbid, Jordan

OPEN ACCESS

Edited by:
Isabelle Bekeredjian-Ding, Paul-Ehrlich-Institut (PEI), Germany

Reviewed by:
Laura Elizabeth Layland-Heni, University Hospital Bonn, Germany
Christian H. K. Lehmann, Universitatsklinikum Erlangen, Germany
Ger van Zandbergen, Paul-Ehrlich-Institut (PEI), Germany

***Correspondence:**
Christian Keller
christian.keller@staff.uni-marburg.de

Specialty section:
This article was submitted to Microbial Immunology, a section of the journal Frontiers in Immunology

Received: *20 February 2021*
Accepted: *21 June 2021*
Published: *05 July 2021*

Citation:
Petermann M, Orfanos Z, Sellau J, Gharaibeh M, Lotter H, Fleischer B and Keller C (2021) CCR2 Deficiency Impairs Ly6C^{lo} and Ly6C^{hi} Monocyte Responses in Orientia tsutsugamushi Infection. Front. Immunol. 12:670219. doi: 10.3389/fimmu.2021.670219

Orientia (O.) tsutsugamushi, the causative agent of scrub typhus, is a neglected, obligate intracellular bacterium that has a prominent tropism for monocytes and macrophages. Complications often involve the lung, where interstitial pneumonia is a typical finding. The severity of scrub typhus in humans has been linked to altered plasma concentrations of chemokines which are known to act as chemoattractants for myeloid cells. The trafficking and function of monocyte responses is critically regulated by interaction of the CC chemokine ligand 2 (CCL2) and its CC chemokine receptor CCR2. In a self-healing mouse model of intradermal infection with the human-pathogenic Karp strain of *O. tsutsugamushi*, we investigated the role of CCR2 on bacterial dissemination, development of symptoms, lung histology and monocyte subsets in blood and lungs. CCR2-deficient mice showed a delayed onset of disease and resolution of symptoms, higher concentrations and impaired clearance of bacteria in the lung and the liver, accompanied by a slow infiltration of interstitial macrophages into the lungs. In the blood, we found an induction of circulating monocytes that depended on CCR2, while only a small increase in Ly6C^{hi} monocytes was observed in *CCR2*$^{-/-}$ mice. In the lung, significantly higher numbers of Ly6C^{hi} and Ly6C^{lo} monocytes were found in the C57BL/6 mice compared to *CCR2*$^{-/-}$ mice. Both wildtype and CCR2-deficient mice developed an inflammatory milieu as shown by cytokine and *inos/arg1* mRNA induction in the lung, but with delayed kinetics in CCR2-deficient mice. Histopathology revealed that infiltration of macrophages to the parenchyma, but not into the peribronchial tissue, depended on CCR2. In sum, our data suggest that in *Orientia* infection, CCR2 drives blood monocytosis and the influx and activation of Ly6C^{hi} and Ly6C^{lo} monocytes into the lung, thereby accelerating bacterial replication and development of interstitial pulmonary inflammation.

Keywords: inflammatory monocytes, scrub typhus (Tsutsugamushi disease), chemokines, rickettsiosis, chemokine receptor (CCR2), interstitial pneumonia

INTRODUCTION

Scrub typhus is a mite-borne, neglected tropical infection caused by the obligate intracellular bacterium *Orientia (O.) tsutsugamushi*. In humans, transmission of *O. tsutsugamushi* during mite bites induces a cutaneous necrosis, the eschar (1), and is accompanied by undifferentiated fever in mild cases. In more severe cases, the infection may progress to interstitial pneumonia, acute respiratory distress syndrome (ARDS), myocarditis, encephalitis or other complications that may be lethal if not treated adequately.

O. tsutsugamushi has long been known to be a potent inducer of monocyte-related chemokines in humans and mice (2–4). Robust evidence supports a macrophage/monocyte tropism for this pathogen in blood and tissue (1, 5, 6) and strong macrophage responses in infected tissues (7, 8). Moreover, *O. tsutsugamushi* infects and replicates in human blood-derived monocytes *ex vivo*, as it does in neutrophils (9, 10).

In the pathogenesis of human scrub typhus, chemokine networks play an important role, and increased plasma concentrations of the chemokines CC chemokine ligand (CCL) 2 (monocyte chemoattractant protein-1), CCL4 (macrophage inflammatory protein-1β) and interleukin (IL)-8 have been associated with disease severity (11).

Chemokines shape the type and extent of monocyte responses. In mice, there are two major subsets of circulating monocytes: First, the "inflammatory" or classical monocytes, identified as $CD11b^+$ $Ly6C^{hi}$ $Ly6G^-$ and expressing the CC chemokine receptor 2 (CCR2) at high levels. These inflammatory monocytes can be rapidly recruited into inflamed tissues. In mice lacking CCR2, a receptor for CCL2 and CCL7, severe defects in recruitment of inflammatory monocytes and tissue macrophages are observed (12–14). Consequently, CCR2 deficiency in mice drastically increases the susceptibility to infection with intracellular bacteria, viruses and protozoan parasites (13, 15–17). Inflammatory monocytes may, on the other hand, mediate pathology in inflammatory diseases such as atherosclerosis, where their absence confers an attenuated phenotype (12), or in the formation of liver abscesses in amebiasis (18).

A second subset of "resident" monocytes is identified as $CD11b^+$ $Ly6C^{lo}$ $Ly6G^-$; these cells express only low levels of CCR2, but high levels of CX_3CR1 (19). $CD11b^+$ $Ly6C^{lo}$ monocytes have a "patrolling" function in and around the vascular endothelium (20). They can rapidly extravasate into inflamed tissue where they follow a typical macrophage differentiation program. Subsequently, they may give rise to M2 type macrophages expressing *arg1*, e.g. in atherosclerosis (21). It was recently shown in a model of sterile hepatic inflammation that $CCR2^{hi}$ monocytes are recruited to injured sites and transition *in situ* to $CX3CR1^{hi}$ $CCR2^{lo}$ monocytes (22).

Recent studies have revealed that there is a substantial degree of plasticity among macrophage subsets. Tissue-resident macrophages such as Kupffer cells, microglia, Langerhans cells and alveolar macrophages are now known to derive from embryonic precursors (23, 24), but circulating blood monocytes can replenish these macrophage populations upon tissue injury later in life (25, 26). Upon exposure to external stimuli, macrophage activation can follow either the "classical" M1 pattern, after exposure to bacteria or interferon (IFN)-γ (27, 28), or the "alternative" M2 pattern, after exposure to IL-4 (29, 30). With an increasing number of polarizing stimuli and subtypes of polarization identified, the M1/M2 paradigm has been challenged, and the need for immunological contextualization was highlighted (31, 32).

While the chemokine CCL2 is produced ubiquitously in many infections, it had long remained unknown whether this chemokine could act over a long distance, or if the bone marrow needed to be locally infected to induce the egress of monocytes. Shi et al. demonstrated that the first critical step is local CCL2 production in the bone marrow: mesenchymal stem cells produce CCL2 in response to very low levels of circulating Toll-like receptor (TLR) ligands and thus trigger release of $Ly6C^{hi}$ $CCR2^+$ monocytes into the bloodstream (33). Thereby, CCR2-mediated signals in bone marrow determine the frequency of $Ly6C^{hi}$ monocytes in the circulation (14).

In the lung of *Orientia*-infected mice, interstitial and peribronchial macrophage lesions have been identified (7). Similarly, in the lung of human patients, the typical finding is an interstitial pneumonia, which seems to be associated with disease severity (34–36). While it was shown that *Orientia* drives M1 responses in the lungs (8), no mechanistic studies on chemokine-driven recruitment of myeloid cells have been provided yet. In the present study, we hypothesized that CCR2 is critical for the development of pulmonary monocyte/macrophage responses and associated bacterial clearance in *Orientia* infection. We reveal a role for CCR2 in formation of interstitial lung lesions, in shaping pulmonary and blood myeloid compartments and local pathogen defense, in a model of self-healing intradermal *Orientia* mouse infection.

METHODS

Animal Experiments

All animal experiments were approved by the Hamburg Authority for Health and Consumer Protection (no. 106/15) and complied with the provisions of the Animal Welfare Act. CCR2-deficient mice on the C57BL/6 background, that were originally created on the 129/Ola background (37, 38), were kindly provided by Prof. Frank Tacke, Department of Hepatology and Gastroenterology, Campus Charité Mitte (CCM)/Campus Virchow-Klinikum (CVK), Charité, Berlin, and backcrossed >10 times to C57BL/6 mice.

Animals were bred and kept in the animal facility of the BNITM Hamburg in individually ventilated cages (IVCs). C57BL/6 wildtype mice were purchased from Charles River Laboratories (Sulzfeld, Germany). Animals were grouped of up to 4 animals per cage. Females were used at the age of 6-12 weeks. Infections with *O. tsutsugamushi* were performed in the BSL3 animal suit at BNITM, Hamburg. Pellet food and water were available to the animals *ad libitum*. Cages, bedding, cellulose paper for nest building, food and water were changed once a week.

Infection of Animals

Infectious stocks of *O. tsutsugamushi* Karp-infected and uninfected L929 cells were stored in liquid nitrogen in 2 ml tubes (Nunc, Thermo Fisher Scientific). For infection, stocks were thawed, reconstituted in RPMI medium, washed twice, taken up in 1 ml PBS and stored on ice until intradermal injection in 1.5 ml Eppendorf tubes. Accordingly, L929 control cells were treated. Before infection, mice were anesthetized with 10 µl/g body weight of a solution containing ketamine (12 mg/ml) and xylazine (1.6 mg/ml). When the animals showed no reflexes, mice were infected intradermally over several sites of the right hind footpad (unilaterally), with a total dose of 5000 spot-forming units (*sfu*) (7).

Collection of Organs

Prior to manipulation, mice received a lethal anesthesia, containing ketamine (12 mg/ml) and xylazine (1.6 mg/ml) at a weight-adapted dose of 15 µl/g body weight. When reflexes were absent, animals were dissected and organs removed. For preparation of lungs, the inferior vena cava was incised for rapid bleeding. The right cardiac ventricle was punctured with an 18G cannula. A button cannula was inserted into the ventricle *via* the puncture site and passed over the pulmonary valve. Subsequently, the lung was perfused through the pulmonary artery with 5 ml PBS. Finally, the lungs were freed of connective tissue and removed together with the proximal trachea. The liver was collected from the abdominal cavity. The organs were stored in 5 ml RPMI in 6-well plates on ice until further processing. Neck dislocation was performed immediately after organ removal. Blood samples collected from the vena cava were centrifuged at 6000 g for 5 minutes, and the serum was transferred to a 1.5 ml tube and stored at -20°C until further processing.

Mandibular Blood Sampling for Flow Cytometry Analysis

By puncturing the submandibular plexus with a lancet, blood was taken using a heparinized capillary tube (20 µl) and immediately purged in 1 ml PBS-filled FACS tube using a 20 µl pipette. A tissue swab was applied onto the puncture site for 30 seconds to avoid possible rebleeding.

Preparation of the Lung for Histology

To maintain the structure of the initially collapsed lungs, the airways were filled with 1% formalin. After irrigation of the pulmonary artery with 5 ml of PBS (Life Technologies, Darmstadt, Germany), the trachea was exposed by a cutaneous longitudinal incision from the thoracic aperture to the mandible and a straight cannula inserted distally between the cartilage clasps. The cannula was fixed with a thread, and the airways were filled *via* this access with 0.7 ml of 1% formalin solution, followed by closure of the trachea with the thread. The lung was removed from the thorax and transferred to a 15 ml tube filled with 10 ml of 1% formalin. All preparations were stored at 4°C until processing by the Mouse Pathology Facility at the Institute of Neuropathology (Prof. Dr. M. Glatzel, University Hospital Hamburg Eppendorf, Germany). Immunohistological staining for IBA1 (ionized calcium binding adapter molecule 1; WAKO, Neuss, Germany) was performed using the Ventana Benchmark XT (Ventana, Tuscon, Arizona, USA), as previously described (7). Sections were recorded with a BZ-9000 Keyence fluorescence microscope.

Co-staining of a lung sample from an *Orientia*-infected C57BL/6 mouse (retrieved on day 14 p.i.) for IBA1 (rabbit-anti-IBA1), *O. tsutsugamushi* (mouse-anti-56kD) and DAPI (Sigma, Darmstadt, Germany) was performed as previously described (7). Images were recorded with an Olympus confocal microscope.

Quantification of Histological Images Using ImageJ

Images were imported into Adobe Photoshop, and areas devoid of tissue, representing empty air-filled space, were selected using the Magic Wand Tool ("Anti-alias" and "contiguous" deselected) using an appropriate tolerance value (usually between 12-20). Selected areas were deleted by menu: Edit > Clear. Resulting images, with empty space as white, were imported in ImageJ. Bronchial areas in images of the Parenchyma were manually erased, and vice-versa. Every image was analysed with the IHC Toolbox Plugin (https://imagej.nih.gov/ij/plugins/ihc-toolbox/index.html), scanning for brown color (representing IBA1 staining) with the H-DAB model. This returns a new separate image with all brown-stained areas extracted on a white background. Both images, the edited source and the extracted brown staining, were converted to monochromatic 8-bit, and an intensity threshold was applied (menu: Image > Adjust > Threshold), with the upper limit a few values below the pure white maximum. This represents every pixel that contains data as black and empty background pixels as white. The black area of both images, the one derived from the source image and the one from the IHC Toolbox scan, was measured by menu: Analyse > Measure. The ratio of the two measurements represents the percentage of the tissue area that is stained in the source image, with all air-filled areas excluded.

Preparation of Blood Samples for FACS Analysis

Peripheral venous blood samples (20 µl) were resuspended in 1 ml of FACS buffer and then centrifuged for 5 min at 322xg and 4°C. The pellet was resuspended in 0.7 ml of erythrocyte lysis buffer (10% 0,17 M TRIS, 90% 0,17 M NH_4Cl pH 7,4), and incubated for 6 minutes at room temperature. The now translucent suspension was diluted with 2 ml of FACS buffer to stop the lysis, and centrifugation was repeated.

Single Cell Suspensions From Lung

The lungs were cut into small pieces using a scalpel, in sterile Petri dishes on ice. The tissue pieces were transferred into 15 ml tubes filled with 3 ml of DNAse (Sigma-Aldrich, Deisenhofen, Germany)/collagenase D (Roche diagnostics, Risch, Switzerland) solution (1:100 collagenase stock solution;
10 µg/mL DNAse I) and incubated in a 37°C water bath for 60 minutes. Every 20 minutes, the samples were sheared 3 times

with a sterile Pasteur pipette. After one hour, the enzyme activity was stopped by addition of 150 µl 0.1 M EDTA (Sigma-Aldrich, Deisenhofen, Germany) sheared again, and incubated for 5 more minutes at 37°C. The tissue samples were then passed *via* a 70 µm Cell Strainer (Becton Dickinson, Heidelberg, Germany) using 2 ml RPMI into a 50 ml tube.

The suspension was centrifuged at 322xg/4°C for 5 minutes and the supernatant discarded. After two more washes with 5 ml of RPMI, the suspensions were taken up in 0.5 ml of RPMI, and leucocytes were counted in a Neubauer counting chamber (Hecht-Assistant, Sondheim, Germany).

Flow Cytometric Analysis

Antibody staining of cell suspension from blood or lungs was done in 5 ml tubes (Sarstedt, Nümbrecht, Germany). Centrifugation was carried out at 322 x g and 4°C for 5 minutes unless otherwise specified. For lungs, 10^8 cells were transferred to one tube. From blood samples, all cells were used. Cells were washed in 2 ml FACS buffer, and incubated with 50 µl Fc-block (BNITM, Hamburg, Germany) for 10 minutes at 4°C. Subsequently, 50 µl of prediluted antibodies (diluted in Fc-block) were added and incubated for 60 minutes at 4°C in the dark. After incubation, cells were washed with 2 ml of FACS buffer. Cells were fixed with 100 µl of 4% paraformaldehyde (Serva, Heidelberg, Germany) in PBS and incubated for 20 minutes at 4°C in the dark. Intermediate storage took place at 4°C in the dark.

Antibodies used for blood panel: FITC-anti-Ly-6C (clone: HK1.4, BioLegend, San Diego, CA, USA); PE-anti-MHCII (clone: M5/114.15.2, Ebioscience); PerCP-Cy5.5-anti-CD11b (clone: M1/70, BD); APC-anti-Ly6G (clone: 1A8, BioLegend). Antibodies used for lung/spleen panel: eFluor®450-anti-CD11b (clone: M1/70, Ebioscience); FITC-anti-MHCII (clone: M5/114.15.2, Ebioscience); PE-anti-Ly6C (clone: HK1.4, BioLegend) or BV510-anti-Ly6C (clone: HK1.4, BioLegend); PerCP-Cy5.5-anti-Ly6G (clone: 1A8, BioLegend); APC-anti-F4/80 (clone: BM8, Ebioscience). Antibodies used to measure CCR2 expression: BV510-anti-CD11b (clone: M1/70, Biolegend); FITC- or PE-anti-Ly6C (clone: HK1.4, BioLegend); APC/Cy7-anti-Ly6G (clone: 1A8, BioLegend); AF700-anti-CCR2 (clone: #475301, R&D).

All samples were analyzed by FACS within 12 hours of fixation. The antibody-labeled cell samples were run on a LSRII. Data analysis was carried out using FlowJo™ 10.06 or 10.07 software (Becton Dickinson; Ashland, Oregon, USA).

In order to quantify the concentration of leukocytes in single cell suspensions from organs, trypan blue-negative cells were counted manually in Neubauer chambers with an inverse light microscope. The entire processed sample - corresponding to 20 µl blood or one lung wing, and resuspended in 200 µl FACS buffer - was analyzed by LSRII; from the "cell gate", the single cell count was then determined using FlowJo software. In case of blood, since 20 µl of blood samples were processed, the cell count obtained was divided by 20 to express results as single cells/µl blood. Using FlowJo, the frequency of each cell population (in %) with respect to all single cells was analyzed and multiplied with the single cell count.

For identification of $CD11b^+$, $Ly6G^+$, $Ly6C^{hi}$ or $Ly6C^{lo}$ populations, the gates were drawn in analogy to previously published reports (14, 39) and considering negative populations in the same sample.

Isolation of DNA and Quantitative Real-Time PCR

Bacterial concentrations in samples from lung (50 mg), liver and spleen (30 mg) were determined by quantitative *traD* qPCR analysis, normalized to the DNA content of the eluate, as described (7). *TraD* qPCR reactions were performed on a 384-well LightCycler 480 (Roche, Mannheim, Germany).

Statistical Analysis

Graphpad Prism 7.0 software was used for statistical analysis. Descriptive statistics show mean +/- SD. Hypotheses were tested by two-tailed t test, by one-way or two-way analysis of variance (ANOVA) with Bonferroni post-correction, or by Mantel-Cox test. A p value of <0.05 was considered significant.

Isolation of mRNA

50 mg of lung tissue were transferred to 100 ml of Trizol (Invitrogen, Karlsruhe, Germany) in 2 ml Precellys tubes (Precellys, Bertin Technologies, Villeurbanne, France) and kept on ice. The tissue was homogenized (Precellys 24, Peqlab, Erlangen, Germany) and immediately frozen at -80°C. For phase separation, the frozen samples were thawed and centrifuged at 11800 x g for 5 min at 4°C. The supernatant was mixed with 0.2 ml of chloroform (Roth, Karlsruhe, Germany) and shaken manually for 15 seconds, followed by centrifugation at 11800 x g/15 min/4°C. The aqueous phase was mixed with 500 µl of isopropanol (Roth, Karlsruhe Germany). After incubation at room temperature (10 min) and centrifugation, (11800 x g/10min/4°C), the pellet was washed and vortexed with 75% ethanol (Roth, Karlsruhe, Germany). After centrifugation (7280 x g/5 min/4°C), the pellet was dissolved in 150 µl RNase-free water (Qiagen, Hilden, Germany) and incubated at 60°C for 12 minutes. The subsequent storage took place at -80°C. DNA digestion with DNAse (RNase-free DNase-Set, Qiagen, Hilden, Germany) was performed before RNA extraction (Rneasy Mini Kit, Qiagen, Hilden, Germany).

For this purpose, 85 µl DNA extract was mixed with 10 µl RDD buffer (DNAse-Set, Qiagen), then 2.5 µl DNAse-stock solution was added and incubated for 10 min at room temperature. Following the Qiagen RNeasy mini kit protocol, the sample was mixed with 350 µl RLT buffer or before 250 µl ethanol 70% was added and the mixture was placed on a column. Centrifugation was carried out at 8000 x g for 15 s at room temperature. The flow was discarded. Then 500 µl of RPE buffer was added over the column and centrifuged for 15 seconds at 8000 × g and room temperature. Another 500 µl of RPE buffer was added and centrifuged for 2 min at 8000 x g and room temperature. The column was placed in a new collection tube and again for a 1 min at the above. conditions centrifuged. the column was then placed in a 1.5 ml safe lock and 50 µl of nuclease-free water was added, again centrifugation for 1 min under the same conditions.

Reverse Transcription and Quantitative Real-Time PCR

The nucleic acid concentration was determined by spectrophotometry (Nanodrop, ThermoFisher Scientific, Waltham MA, USA), and the sample was diluted for reverse transcription performed by using 2 µg RNA diluted in 10 µl nuclease-free water for further analysis. The high-capacity cDNA reverse transcription kit (Life Technologies, Waltham MA, USA) was used for reverse transcription in a Thermocycler (Primus advanced, Peqlab, Erlangen, Germany) of 10 µl RNA sample as recommended by the manufacturer (25°C, 10 min; 37°C, 120 min; 85°C, 5 min, storage at 4°C).

Gene expression analysis by quantitative real-time PCR was carried out on a 384-well LightCycler 480II (Roche Diagnostics, Risch, Switzerland). The 10 µl reactions (HotStar Taq, Qiagen, Germany) contained 1 µl cDNA template in the presence of 300 nM sense and antisense primers (see **Table 1**), 1mM additional $MgCl_2$, 200 mM dNTPs, 0.25 U taq polymerase and 0.1 µl SYBR Green 1:1000 in DMSO (Sigma, Germany). Reaction condition were 95°C, 15 min; touchdown (6 cycles): 95°C, 30 s - 64>58°C, 40 s - 72°C, 30 s; amplification (29 cycles): 95°C, 30 s - 58°C, 40 s, 72°C, 30 s; melting curve: 95°C, 1 min - 67°C > 95°C [1°C/step] - 40°C, 20 s. Samples were run as technical duplicates; when not meeting a Cp standard deviation of <1, the measurement was repeated.

Gene Expression Analysis

The induction of gene expression was calculated as n-fold induction using the Cp-value of the respective target genes and the reference gene *rps9*. The following formula was used:

$$\frac{2^{(\text{Cp target [non - infected control]} - \text{Cp target [infected, day x]})}}{2^{(\text{Cp } rps9 \text{ [non - infected control]} - \text{Cp } rps9 \text{ [infected, day x]})}}$$

The efficiency of target and reference amplification was set to 2, and as controls, the average of mean Cp (both target and *rps9*) from non-infected animals (day 0) was used.

Scoring of Mice

Mice were weighed using a digital scale (Denver-Instrument, Göttingen, Germany). The scoring was based on clinical and behavioral symptoms: 1: neck fur ruffled, loss of curiosity; 2: back fur ruffled, acute tiredness; 3: complete fur ruffled, heavy breathing, distended abdomen, apathy, hunched posture.

TABLE 1 | Primers for gene expression analysis.

Target gene	Primer sequence	Source
***arg1* s (sense)**	5'-TCCAGAAGAATGGAAGAGTCAG-3'	this study
***arg1* as (antisense)**	5'-CAGATATGCAGGGAGTCACC-3'	this study
***il-4* s**	5'-GCATTTTGAAGAGGTCACAGG-3'	(40)
***Il-4* as**	5'-TATGCGAAGCACCTTGGAAGC-3'	(40)
***inos* s**	5'-TGGTGGTGACAAGCACATTTG-3'	(18)
***inos* as**	5'-AAGGCCAAACACAGCATACC-3'	(18)
***ccl2* s**	5'-TCTCTCTTCCTCCACCACCA-3'	(18)
***ccl2* as**	5'-CGTTAACTGCATCTGGCTGA-3'	(18)
***ifn-γ* s**	5'- GATGCATTCATGAGTATTGCCAAGT -3'	(18)
***ifn-γ* as**	5'- GTGGACCACTCGGATGAGCTC -3'	(18)
***tnf-α* s**	5'-GTTTGCTACGACGTGGGCT-3'	(18), modified
***tnf-α* as**	5'-CCAAATGGCCTCCCTCTCA-3'	(18), modified
***rps9* s**	5'- CCGCCTTGTCTCTCTTTGTC -3'	(18)
***rps9* as**	5'- CCGGAGTCCATACTCTCCAA -3'	(18)

RESULTS

IBA1$^+$ Macrophages Are Host Cells for *O. tsutsugamushi* in the Lung

Macrophages, which can be histologically identified by IBA1 (ionized calcium binding adapter molecule 1)-specific staining (41), represent a major component of induced pulmonary infiltrates in mouse infections with *Orientia* (7, 42). In the lungs of infected mice, we identified intracellular *Orientia* in IBA1$^+$ macrophages (**Figure 1A**). Yet, the mechanisms of macrophage recruitment to the lung, as well as their roles in bacterial dissemination and antibacterial defense remains unknown in *Orientia* infection.

CCR2$^{-/-}$ Mice Show Delayed Bacterial Clearance, Symptom Development and Macrophage Invasion Into Lungs

The C-C chemokine receptor CCR2 is known to be vital for the recruitment of macrophages to inflamed tissues (13), *via* mobilization of inflammatory monocyte precursors from the bone marrow to the blood (14). Thus, we investigated whether CCR2-dependent recruitment of macrophages and monocytes is required for systemic dissemination of *O. tsutsugamushi* and protection. First, we assessed bacterial dissemination to lung and liver, clinical course and lung histopathology in CCR2-deficient and C57BL/6 wild type mice. The bacterial concentrations on day 10 p.i. in lungs (**Figure 1B**) and liver (**Figure S1**) did not differ between *CCR2*$^{-/-}$ and wildtype mice, suggesting an unimpeded dissemination from the cutaneous inoculation site to internal organs. However, *CCR2*$^{-/-}$ mice had higher bacterial concentrations on day 14 and 17 p.i. in both organs, suggesting an impaired clearance of *O. tsutsugamushi* in the absence of CCR2-dependent inflammatory monocytes (**Figures 1B**, **S1**). Also, *CCR2*$^{-/-}$ mice showed delayed onset and delayed recovery from symptom development (**Figure 1C**). This delay in the course of symptoms and bacterial clearance in *CCR2*$^{-/-}$ mice also correlated with a delayed pulmonary influx of IBA1$^+$ macrophages to the lungs (**Figure 1D**). Thus, bacterial clearance, onset and recovery from symptoms and pulmonary macrophage inflammation (as investigated by histopathology) were accelerated by a CCR2-dependent cell population in our model of *O. tsutsugamushi* infection.

Defective Mobilization of Ly6C^{hi} and Ly6C^{lo} Blood Monocytes in *CCR2*$^{-/-}$ Mice During *O. tsutsugamushi* Infection

We next investigated whether *O. tsutsugamushi*-infected *CCR2*$^{-/-}$ mice show defective mobilization of inflammatory monocytes to the blood. To that end, the expression of CD11b, Ly6C and Ly6G on PBMCs was measured by FACS (for gating strategy see **Figure 2A**). To identify inflammatory monocytes, we analyzed

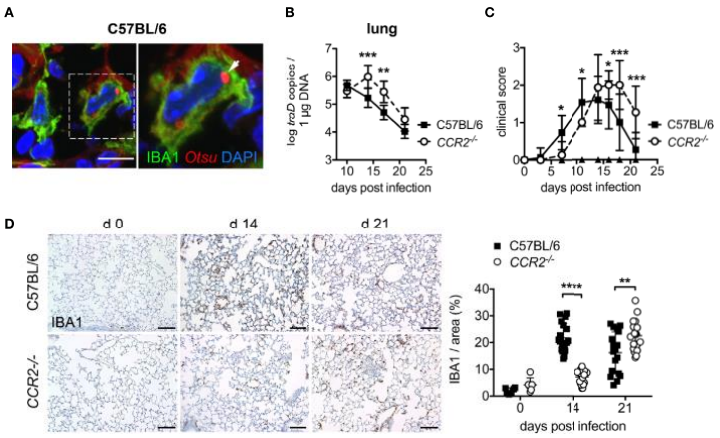

FIGURE 1 | CCR2 deficiency delays bacterial clearance of *O. tsutsugamushi* and macrophage infiltration in the lung. **(A)** Immunofluorescence staining for *O. tsutsugamushi* (*Otsu*, anti-56 kD mAb, red) and macrophages (IBA1, green) from the lungs of an infected C57BL/6 mouse (day 14 p.i.) reveals intracellular *Orientia* organisms. Blue, DAPI. Scale bar: 10 µm. **(B)** *CCR2*$^{-/-}$ or C57BL/6 mice were infected with 5,000 sfu *O. tsutsugamushi* in the hind footpad. Per genotype, n=3 mice were sacrificed on days 10, 14, 17 and 21, and bacterial concentrations were quantified from the lungs by *traD*-specific qPCR. Data from two independent experiments were pooled; shown are means of bacterial concentrations from organs of n=2x3 = 6 mice per genotype and time point ± SD. **(C)** *CCR2*$^{-/-}$ or C57BL/6 mice (n=5 mice per genotype) were infected with 5,000 sfu *O. tsutsugamushi* in the hind footpad. Clinical scores were recorded on days 0, 3, 7, 11, 14, 16, 18 and 21. Shown are pooled results from three independent experiments (means of n=15 infected animals per group ± SD). **(D)** *CCR2*$^{-/-}$ or C57BL/6 mice were infected with 5,000 sfu *O. tsutsugamushi* in the hind footpad. N=3 mice per genotype and timepoint were sacrificed on days 14 and 21, and macrophages were stained by immunohistochemistry for IBA1 in histological sections from lungs. Representative histological images are shown from parenchyma areas. Scale bar: 100 µm. The IBA1^{+} area was quantified (6 areas per lung section from n=3 infected [day 14, 21] and n=1 uninfected [day 0] mice per genotype; mean ± SD). *p < 0.05; **p < 0.01; ***p < 0.001; ****p < 0.0001 by two-way ANOVA.

the percentage of Ly6C^{hi} cells among all CD11b^{+} Ly6C^{+} cells and enumerated them (**Figures 2B, C**). Prior to infection, wildtype animals had an about 5-fold higher percentage of Ly6C^{hi} cells, compared to CCR2-deficient mice (**Figures 2B, C**). This percentage increased in wildtype mice from day 10 on, to about 80% on day 17 p.i. (**Figure 2C**). Interestingly, *CCR2*$^{-/-}$ mice also displayed an albeit reduced increase in their percentage of Ly6C^{hi}/Ly6C^{+} monocytes in blood (**Figures 2B, C** left panel). Higher numbers of Ly6C^{hi} inflammatory monocytes were measured from day 14 p.i. in wildtype mice, giving rise to a 3-4-fold induction in blood in absolute numbers (**Figure 2C**, right panel). Notably, despite a drop in percentage (**Figures 2B, C** left panel), we also observed an induction of absolute numbers of CD11b^{+} Ly6C^{lo} monocytes from day 17 p.i. that was CCR2-dependent (**Figure 2D**). Contrarily, the induction of CD11b^{+} Ly6G^{+} neutrophils from day 14 p.i. was independent of CCR2 (**Figure 2E**).

Thus, wildtype mice showed an induction of both CD11b^{+} Ly6C^{hi} and CD11b^{+} Ly6C^{lo} monocytes in blood during infection with *O. tsutsugamushi* in C57BL/6 mice. In *CCR2*$^{-/-}$ mice, contrarily, a very small and delayed induction that was demonstrable only in the relative amount of Ly6C^{hi}/Ly6C^{+} monocytes was found. Blood monocytosis during *O. tsutsugamushi* infection is thus largely CCR2-dependent.

Reduced Influx of Ly6C^{hi} Monocyte Subsets Into the Lung of *CCR2*$^{-/-}$ Mice During *O. tsutsugamushi* Infection

Histopathology of lung samples suggested at delayed influx of macrophages to the lung in CCR2 deficiency (**Figure 1D**). In order to phenotypically and quantitatively characterize pulmonary inflammation, we analyzed Ly6C^{hi}, Ly6C^{lo} and Ly6G^{+} cells (gating strategy in **Figure 3A**). In C57BL/6 mice, the percentage of Ly6C^{hi} among all CD11b^{+} Ly6C^{+} cells was significantly higher compared to *CCR2*$^{-/-}$ mice on day 0, but not during *Orientia* infection: from day 10 p.i., *CCR2*$^{-/-}$ mice displayed similar percentages of Ly6C^{hi} cells in the lung (**Figures 2B, C** right panel). With view to absolute numbers, however, we found clear differences between the two genotypes: C57BL/6 mice showed a much stronger induction to 4-8-fold higher numbers of Ly6C^{hi} monocytes in their lungs compared to *CCR2*$^{-/-}$ mice, peaking at day 14 p.i. (**Figure 3C**, right panel). Over the entire course of *Orientia* infection, these differences were highly significant. Also, >90-95% of the CD11b^{+} Ly6C^{hi} cells of both genotypes expressed F4/80, suggesting that the vast majority of this population were macrophages (**Figure S2A**). The expression of MHCII by CD11b^{+} Ly6C^{hi} cells was between 10-20% in uninfected mice and rose to >80-90% during infection,

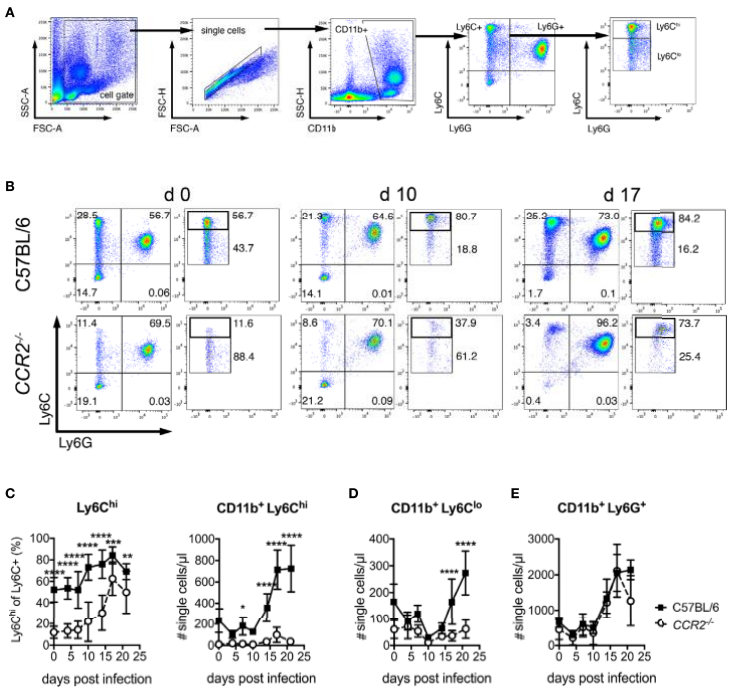

FIGURE 2 | Induction of Ly6C^{hi} and Ly6C^{lo} monocytes in peripheral blood depends on CCR2 during *O. tsutsugamushi* infection. C57BL/6 and *CCR2*$^{-/-}$ mice were infected i.d. with *O. tsutsugamushi*. From venous blood samples retrieved from infected animals on days 4, 7, 10, 14, 17 and 21 p.i., peripheral blood mononuclear cells were stained for CD11b, Ly6C and Ly6G and analyzed by FACS. **(A)** Gating strategy for blood neutrophils and monocyte subsets. **(B)** Analysis of Ly6C and Ly6G expression on CD11b^{+} cells. For Ly6C^{hi} and Ly6C^{lo} cells, percentages are expressed as % of pre-gated CD11b^{+} Ly6C^{+} cells. Representative dotplots from d 0, d 10 and d 17 are shown. **(C)** Percentages of Ly6C^{hi}/Ly6C^{+} cells (left) and concentrations of CD11b^{+} Ly6C^{hi} cells per µl blood. **(D)** Concentrations of CD11b^{+} Ly6C^{lo} and **(E)** CD11b^{+} Ly6G^{+} cells per µl blood at the indicated days p.i. Shown are pooled results from three independent experiments (mean ± SD), with n=4 animals per experiments (values from n=12 animals per genotype and time point). *p < 0.05; **p < 0.01; ***p < 0.001, ****p < 0.0001 by two way-ANOVA.

and we observed a faster upregulation of MHCII in C57BL/6 mice compared to *CCR2*$^{-/-}$ mice on day 10 p.i. (**Figure S2B**).

Contrarily, the numbers of neutrophils in the lung did not differ between both genotypes on days 0, 10, 14 and 21 p.i.; they increased comparably and were only slightly higher in *CCR2*$^{-/-}$ mice on day 17 p.i. (**Figure 3D**). These data suggest that recruitment of CD11b^{+} Ly6C^{hi} monocytes/macrophages to the lung requires CCR2. CCR2 however did not contribute to the recruitment of neutrophils to the lung.

Impaired Pulmonary Ly6C^{lo} Monocytes in the Lung of *CCR2*$^{-/-}$ Mice During *O. tsutsugamushi* Infection

We also observed a prominent Ly6C^{lo} population in the CD11b^{+} Ly6C^{+} gate. Hypothesizing that these cells were also mainly macrophages, we investigated expression of the macrophage marker F4/80. Between 80-90% of pre-gated Ly6C^{lo} cells expressed F4/80 prior to infection (**Figure 4A**), suggesting a macrophage population. The percentage decreased to 40-50% on day 10 p.i., but increased again to 70-80% after day 14 p.i. Percentages of F4/80^{+} cells did not differ significantly between C57BL/6 and *CCR2*$^{-/-}$ mice (**Figure 4A**, middle panel). While the absolute numbers of pulmonary CD11b^{+} Ly6C^{lo} F4/80^{+} macrophages were comparable in both genotypes on day 0, they increased significantly in C57BL/6 mice on days 10, 14, 17 and 21 p.i. compared to *CCR2*$^{-/-}$ mice (**Figure 4A**, right panel). MHCII expression was found on 20-40% of Ly6C^{lo} cells on day 0, but the percentage increased to about 80-90% on days 14, 17 and 21 p.i. (**Figure 4B**, left and middle panels), suggesting an activated macrophage phenotype. Again, significantly higher numbers of CD11b^{+} Ly6C^{lo} MHCII^{+} cells were found in C57BL/6 mice (**Figure 4B**, right panel).

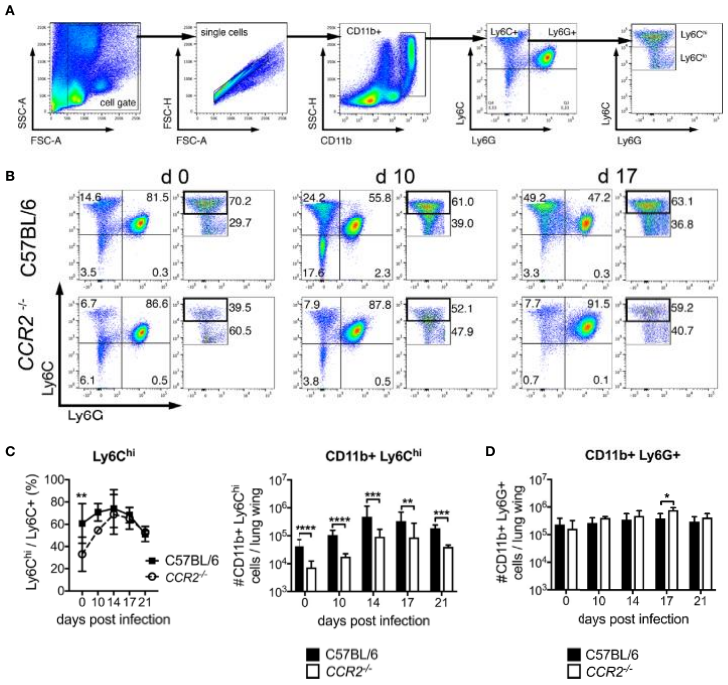

FIGURE 3 | CCR2 drives expansion of Ly6C^{hi} monocyte but not granulocyte populations in the lung during infection with *O. tsutsugamushi*. CCR2-deficient or C57BL/6 mice were infected with 5,000 sfu *O. tsutsugamushi* in the hind footpad. On the indicated days post infection, animals were sacrificed (n=3 per genotype and timepoint), and pulmonary cells were analyzed for expression of CD11b, Ly6C and Ly6G by FACS. **(A)** Gating strategy for pulmonary neutrophils (Ly6G$^+$) and monocyte (Ly6C$^+$) subsets. **(B)** Representative dotplots from d 0, d 10 and d 17 p.i. **(C)** Percentages of Ly6C^{hi}/Ly6C$^+$ cells (left) and absolute numbers of CD11b$^+$ Ly6C^{hi} cells per lung wing (right). **(D)** Absolute numbers of CD11b$^+$ Ly6G^{hi} cells per lung wing. Shown are pooled results from two independent experiments, i.e. from a total of n=6 mice per genotype and timepoint; mean ± SD. *p < 0.05; **p < 0.01; ***p < 0.001, ****p < 0.0001 by two way-ANOVA.

A co-expression analysis showed that during *Orientia* infection, MHCII was mostly expressed by F4/80$^+$ cells (**Figure 4C**, left panels). Also, the F4/80/MHCII double-positive macrophage population increased earlier in wildtype mice. Again, *CCR2*$^{-/-}$ mice did not have a defect in upregulating expression of F4/80 and MHCII on Ly6C^{lo} cells (**Figure 4C**, upper right panel), but the population was 5-10-fold larger in wildtype mice compared to *CCR2*$^{-/-}$ mice (**Figure 4C**, lower right panel).

Although it is possible that the Ly6C^{lo} monocytes developed from the highly CCR2-expressing Ly6C^{hi} monocytes, as previously suggested (22, 43), it is also possible that their recruitment occurred directly *via* CCR2-dependent mechanisms. To confirm observations that Ly6C^{lo} cells also do express CCR2 (44), we measured expression of CCR2 on Ly6C^{hi} and Ly6C^{lo} blood monocytes (**Figures S3A–D**). Ly6C^{lo} monocytes of C57BL/6 mice had a higher MFI in CCR2 staining than cells from *CCR2*$^{-/-}$ mice or unstained controls, demonstrating their expression of CCR2 at low levels (**Figures S3C, D**).

Thus, efficient recruitment of both Ly6C^{hi} and Ly6C^{lo} monocyte/macrophages to the lung of *Orientia*-infected mice required CCR2. Contrarily, there was no defect in the influx of Ly6G$^+$ neutrophils in *CCR2*$^{-/-}$ mice. The defect in CCR2-dependent monocyte/macrophage recruitment paralleled the impaired bacterial clearance in *CCR2*$^{-/-}$ mice.

CCR2 Is Neither Required for Efficient Expansion of Ly6C^{hi} and Ly6C^{lo} Populations nor Bacterial Clearance in the Spleen

The induction of a small population of Ly6C^{hi} monocytes in the blood and the influx of some Ly6C^{hi} and Ly6C^{lo} monocytes/macrophages to the lungs of *CCR2*$^{-/-}$ mice was surprising, suggesting a CCR2-independent source of these cells. It was

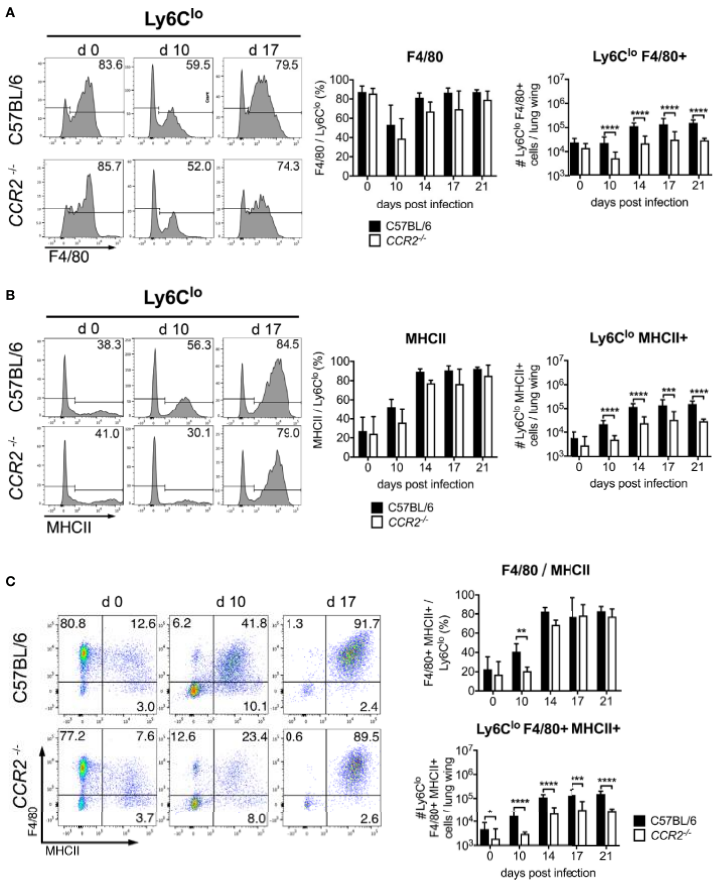

FIGURE 4 | CCR2 is required for efficient recruitment of activated Ly6C^{lo} monocytes to the lung during infection with *O. tsutsugamushi*. *CCR2*$^{-/-}$ or C57BL/6 mice were infected as in **Figure 3.** On CD11b^{+} Ly6C^{lo} cells from the lung, the expression of F4/80 **(A)** and MHCII **(B)** was measured by FACS. Shown are representative histograms from d 0, d 10 and d 17 p.i. (left panels), percentages of marker-positive Ly6C^{lo} cells (middle panels) and absolute numbers per lung wing (right panels). **(C)** Co-expression of F4/80 and MHCII on CD11b+ Ly6C^{lo} cells. Representative dotplots from d 0, d 10 and d 17 (left), percentages (upper right) and absolute numbers per lung wing (lower right panel). Data were pooled from 2 independent experiments (n=6 mice per genotype and time point, mean ± SD). $^{*}p < 0.05$; $^{**}p < 0.01$; $^{***}p < 0.001$, $^{****}p < 0.0001$ by two way-ANOVA.

shown that the spleen can serve as an alternative reservoir for Ly6C^{hi} monocytes, derived from local progenitors, that can be deployed to distant sites such as the heart (45, 46). We therefore investigated the Ly6C^{hi} monocyte population in the spleen of *Orientia*-infected mice. A difference in percentages of Ly6C^{hi}/Ly6C cells and in the size of the Ly6C^{hi} monocyte population was found only prior to infection: During *Orientia* infection, as assessed on days 10, 14, 17 and 21 p.i., *CCR2*$^{-/-}$ mice showed no significant differences to the wildtype regarding the percentages of Ly6C^{hi}/Ly6C^{+} cells, and they also expanded absolute numbers of CD11b^{+} Ly6C^{hi} cells to the same extent as C57BL/6 mice (**Figures S4A, B**). Interestingly, the percentage of Ly6C^{hi} cells dropped more rapidly than in the lung, from about 80% on day 14 p.i. to about 40% on day 21 p.i. This was associated with a normal clearance of *Orientia* from the spleen of *CCR2*$^{-/-}$ mice as shown by qPCR, with no differences to the

C57BL/6 wildtype (**Figure S4C**). Also, no gross defects in the size of Ly6C^{lo} monocyte and Ly6G^{+} neutrophil populations were observed in *CCR2*$^{-/-}$ mice (**Figures S4D, E**).

Thus, a normal expansion of Ly6C^{hi} monocytes in the spleen of *CCR2*$^{-/-}$ mice showed that recruitment of Ly6C^{hi} monocytes *via* CCR2 from the bone marrow to the spleen was not required, in contrast to what we observed in the lung (**Figures 3** and **4**). This expanded Ly6C^{hi} population could potentially constitute an alternative source for monocytes released to the blood or recruited to the lung.

The Establishment of an Inflammatory Cytokine Milieu in the Lung Is Delayed in *CCR2*$^{-/-}$ Mice

In order to characterize the cytokine milieu in lung tissue, we measured transcription of *inos*, *tnf-α*, *ifn-γ* (considered as M1-associated genes) and *il-4* and *arg1* (considered as M2-associated genes) as well as *ccl2* mRNA by quantitative real-time PCR. All genes were up-regulated in both genotypes (**Figure 5**). However, a significant induction of IFN-γ with respect to the baseline transcription level was delayed from day 10 p.i. to day 14 (**Figure 5A**), in *inos* and *tnf-α* from day 14 to day 17 (**Figures 5B, C**) in *CCR2*$^{-/-}$ mice. Interestingly, M2-associated genes were also induced in both genotypes: Again, the peak of *il-4* transcription was delayed from day 10 to day 14 p.i. (**Figure 5D**) in *CCR2*$^{-/-}$ mice, and the peak of *arg1* transcription was even delayed from day 14 p.i. to day 21 p.i. (**Figure 5E**). In general, transcription of *ifn-γ*, *inos* and *ccl2* mRNAs were significantly increased in *CCR2*$^{-/-}$ mice on single days indicated (**Figures 5A, B, F**). This suggests that the development of an inflammatory cytokine milieu is delayed by several days in the absence of CCR2. The delay was consistent with the delayed influx of macrophages to the lungs (**Figures 1**, **3**).

CCR2 Drives Early Infiltration of Macrophages to Lung Parenchyma, but Not Accumulation of Macrophages in BALT

Last, we were interested whether CCR2 influences the histological localization of macrophages in the lung during acute *O. tsutsugamushi* infection. To that end, we performed immunohistochemistry for the macrophage marker IBA1 on FFPE sections of lung tissue. We observed that the parenchyma of wildtype mice was infiltrated by IBA^{+}-positive macrophages on day 14 p.i., when the maximal bacterial concentration in lung tissue was measured. However, this parenchymal infiltration was observed to a much lesser degree in *CCR2*$^{-/-}$ mice (**Figure 6**, upper row). We quantified the IBA^{+}-positive area in 6 randomly selected details from 3 mice in both genotypes by imaging software, and found that the IBA^{+}-positive area in lung parenchyma was significantly larger in C57BL/6 compared to *CCR2*$^{-/-}$ mice (**Figure 6**, upper row). We also observed that this effect was restricted to the parenchyma, since the peribronchial BALT areas were similarly infiltrated by macrophages in both genotypes. Indeed, quantification showed that IBA1^{+} areas in BALT structures did not differ significantly between genotypes (**Figure 6**, lower row). However, on day 21 p.i. (data not shown), infiltration of lung parenchyma was also found in

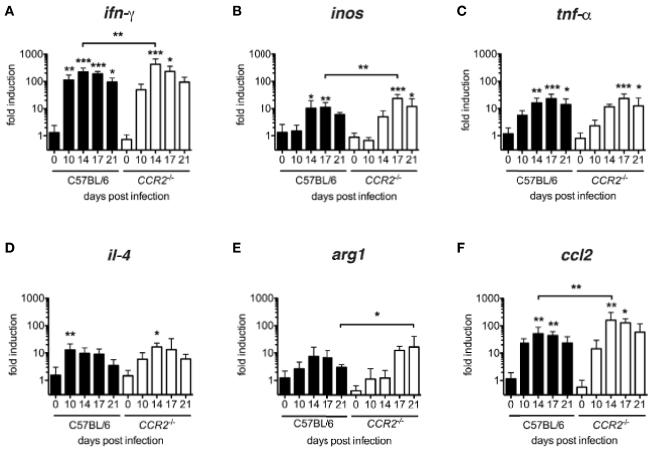

FIGURE 5 | Delayed development of inflammatory milieu in lungs of *O. tsutsugamushi CCR2*$^{-/-}$ mice. *CCR2*$^{-/-}$ and C57BL/6 mice were infected with 5,000 sfu *O. tsutsugamushi* i.d. and sacrificed on days 0, 10, 14, 17 and 21 p.i. From homogenates of lung tissue, transcription of *ifn-γ*, *inos* and *tnf-α*, *il-4*, *arg1* and *ccl2* mRNA was measured by real-time PCR from tissue lysates and expressed as -fold induction at the indicated time points p.i. **(A–F).** Shown are pooled results from two independent experiments (total of n=6 mice per genotype and timepoint; mean ± SD). *p < 0.05; **p < 0.01; ***p < 0.001 by one-way ANOVA.

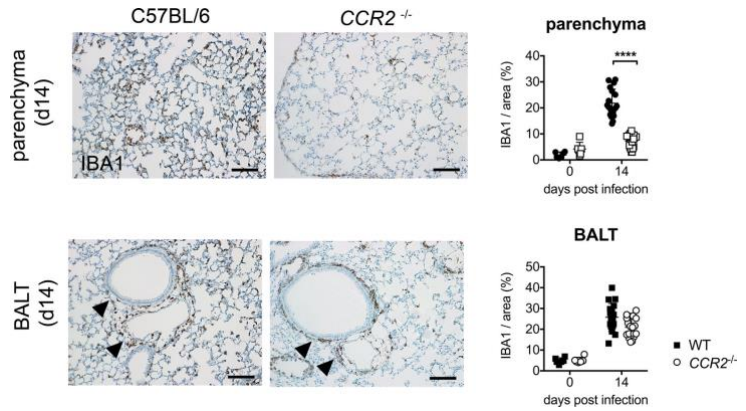

FIGURE 6 | CCR2-dependent macrophage infiltration in lung parenchyma rather than peribronchial BALT. *CCR2*$^{-/-}$ and C57BL/6 mice were infected with 5,000 sfu *O. tsutsugamushi* i.d. and sacrificed on day 14 p.i. (n=3 mice per genotype). Macrophages were stained by immunohistochemistry for IBA1 in histological sections from lungs. Representative histological images are shown from parenchyma (upper row, part of the data are shown in **Figure 1D**) and peribronchial BALT areas (lower row). Scale bar: 100 µm. The IBA1^{+} area was quantified separately in parenchyma and BALT areas (6 areas per lung section from n=3 infected and n=1 uninfected mice per genotype; mean ± SD). ****p < 0.0001 by two-way ANOVA.

CCR2$^{-/-}$ mice, suggesting that CCR2-independent signals compensate this early defect and allow a later infiltration of macrophages to the pulmonary parenchyma.

Taken together, the present study investigated for the first time the mechanism of CCR2-dependent recruitment of monocytes to peripheral blood and lung tissue in a new mouse model of self-healing *O. tsutsugamushi* infection. We showed that clearance of *O. tsutsugamushi* was significantly less effective and delayed in the absence of CCR2 in the lung (and also liver), but *CCR2*$^{-/-}$ mice were eventually able to reduce the infection. CCR2 was required for mobilization of monocytes to the blood and enhanced the influx of Ly6C^{hi} monocytes, most of which developed an activated macrophage phenotype, into the lung. Unexpectedly, there was also a clear dependence of the pulmonary Ly6C^{lo} monocyte/macrophage population on CCR2, while neutrophils were unaffected in number. We could also show that early interstitial infiltration of the lung parenchyma by IBA1^{+} macrophages was CCR2-dependent, while development of peribronchitis was CCR2-independent. In contrast, expansion of Ly6C^{hi} and Ly6C^{lo} populations and bacterial clearance in the spleen were not affected by CCR2 deficiency. Our data suggest that CCR2 orchestrates the temporospatial recruitment and activation of monocytes and macrophages to the lungs, thus contributing locally to the reduction of *O. tsutsugamushi* infection.

DISCUSSION

Inflammatory monocytes, phenotyped as CD11b^{+} Ly6C^{+} Ly6G^{-} in mice, have been implicated in the defense against bacterial, viral, fungal and protozoal pathogens. Their emigration from the bone marrow to the circulation is mediated by interaction of CCL2 (MCP-1) with the chemokine receptor CCR2 (14), which is also highly expressed by CD11b^{+} Ly6C^{+} monocytes (47). Guided by the observations that CCL2 (MCP-1) is strongly induced by *O. tsutsugamushi* (2–4), that *Orientia* is associated with monocytes or monocyte-like cells in eschar lesions and peripheral blood (1, 6) and grows within monocytes (10), we investigated the role of CCR2 in monocyte responses in a murine model of self-healing, i.d. *Orientia* infection.

First, we detected *Orientia* in IBA1^{+} macrophages in the lung, which are an important component of pulmonary inflammation (7). While it is known that *Orientia* infects monocytic/macrophage-like cells and dendritic cells in the skin (1), the nature of its host cell involved in systemic dissemination is not known. Several studies suggested that CD11b^{+} or Ly6C^{+} monocytes, as host cells for intracellular pathogens including *Toxoplasma gondii*, *Burkholderia pseudomallei* or *L. monocytogenes*, are responsible for the pathogens' dissemination to other organs, e.g. the brain (48–50). While we had initially suspected that inflammatory monocytes, which might later differentiate into macrophages, could mediate the dissemination of *Orientia* to organs distant from the inoculation site, this hypothesis had to be rejected with view to the equal or even increased bacterial concentrations in *CCR2*$^{-/-}$ mice in lung, liver and spleen. Given the absence of increased blood monocytosis and the onset of macrophage influx in lung tissue around day 10 p.i., it is unlikely that CCR2-dependent mechanisms play a role in bacterial clearance before that time point. However, we cannot exclude that CCR2

deficiency may influence bacterial replication by some innate mechanism in this early phase.

Several studies have underlined the importance of CCR2-dependent recruitment of inflammatory cells for the control of intracellular pathogens: *CCR2*$^{-/-}$ mice were significantly more susceptible to i.v. infection with *Listeria* (13), i.v. infection with *M. tuberculosis* (15), s.c. infection with WNV (16), intranasal infection with HSV (51) and *Histoplasma capsulatum* (52), and oral or i.p. infection with *Toxoplasma* (53, 54). Contrarily to these intracellular pathogens, our data show that *Orientia* is unique in that CCR2 was not required to confer protection in our intradermal infection model. As a limitation to this study, we cannot exclude that other inoculation routes (e.g. i.v.), higher infection doses or infections in male mice – male mice express higher levels of CCR2 than females in non-classical splenic monocytes (55) – would produce a different phenotype. Also, the role of CCR2 was not investigated in functional assays.

Inflammatory monocytes may influence susceptibility to infection in at least two ways: (1) by participating in antimicrobial defense, thus reducing bacterial replication, or (2) by increasing immunopathology. In our i.d. model of *Orientia* infection, we showed that CCR2 was required to reduce infection in the lung. *CCR2*$^{-/-}$ mice showed significantly reduced recruitment of CD11b^{+} Ly6C^{hi} and Ly6C^{lo} monocytes to the lungs, a delayed infiltration of IBA1^{+} cells to the lung parenchyma, a delayed development of the inflammatory cytokine milieu, and delayed clinical recovery. However, none of the *CCR2*$^{-/-}$ mice succumbed to the infection by day 21 p.i. Of note, there was no defect of bacterial clearance in the spleen, where an unimpaired expansion of CD11b^{+} Ly6C^{hi} and Ly6C^{lo} monocytes was found in *CCR2*$^{-/-}$ mice. The results suggest that small but eventually sufficient numbers of monocytes can be recruited in the absence of CCR2 in *Orientia* infection, either from other organs than the bone marrow, perhaps the spleen, or *via* other receptors. These CCR2-independent mechanisms of antimicrobial defense are sufficient to protect against *Orientia*.

We provide experimental evidence that the pulmonary interstitial IBA1^{+} macrophage inflammation was CCR2-dependent, while the peribronchially infiltrating macrophages appeared in a CCR2-independent fashion. These cells could be an alternative source of macrophages that later migrate into the lung parenchyma. In fact, not all tissue monocytes or macrophages that expand during infection are derived from blood monocytes that are recruited from the bone marrow *via* CCR2: A seminal study by Jenkins et al. demonstrated, in the context of a nematode infection, that macrophages can proliferate locally in the pleural cavity, independent from bone marrow, in response to IL-4 (56). Indeed, we measured a significant increase of local *il-4* mRNA transcription in the lung on day 14 p.i. in *CCR2*$^{-/-}$ mice, albeit later than in wildtype mice. It will therefore be of interest to study the mechanisms of bone marrow-independent macrophage inflammation in *Orientia* infection in the future, e.g. the role of IL-4-driven local proliferation or recruitment from the spleen.

It is interesting to note that the induction of Th2 cytokines appears to depend on the infection route: In the i.v. infection model of *O. tsutsugamushi* Karp that allows rapid dissemination to the organs without passing through the lymph node, transcription of *il-4* and *il-13* mRNA was found suppressed and thus interpreted as an impaired Th2 response (57). In lungs of i.d. infected mice, however, Soong et al. detected IL-13 besides TH1-related cytokines, suggesting a mixed Th1/Th2 response (58). Our data demonstrate that CCR2 deficiency did not completely shift polarization towards one pole in *Orientia* infection, but rather delayed the afore-mentioned mixed phenotype. This is different from *Cryptococcus neoformans* infection where CCR2 deficiency shifted the polarization completely from Th1 to Th2 (59). Our results show that, in the i.d. infection model, the CCR2-independent macrophage response, albeit delayed, is eventually sufficient to control *Orientia* infection in the lung.

While we initially expected that abrogation of CCR2 would reduce primarily the Ly6C^{hi} inflammatory monocytes, we found that also the Ly6C^{lo} monocytes were affected in various ways during *Orientia* infection: In CCR2-deficient animals, *Orientia* infection induced significantly lower concentrations of Ly6C^{lo} monocytes in peripheral blood and the lungs, and also the expression of MHCII and F4/80 by pulmonary Ly6C^{lo} monocytes was significantly decreased during infection in *CCR2*$^{-/-}$ mice.

For Ly6C^{hi} inflammatory monocytes, the role of CCR2 in regulating the circulation of inflammatory monocytes is well understood. Ly6C^{hi} inflammatory monocytes express CCR2 at high levels (44, 47, 60). The expression of CCR2 mediates their egress from the bone marrow to the blood circulation, in response to local CCL2 production by mesenchymal stem and progenitor cells which in turn respond to low concentrations of circulating TLR ligands (14, 33). We now show that during *Orientia* infection, CCR2 was required not only to elicit a systemic Ly6C^{hi} inflammatory monocyte response, but also to induce peripheral Ly6C^{lo} monocytosis and for the induction of a pulmonary Ly6C^{lo} monocyte population. Notably, induction of monocyte responses and bacterial clearance were independent of CCR2 in the spleen in our model. The spleen was shown to provide a large reservoir of undifferentiated monocytes that assemble in clusters in the cords of the subcapsular red pulp (45). From here, they can rapidly exit and deploy to inflamed tissues in a CCR2-independent fashion. These monocytes can derive from splenic common monocyte progenitors (cMoP's), a highly proliferative cell type that may give rise to several monocyte subsets and macrophages (46). For clearance of *Orientia* from the spleen, these local splenic mechanisms appeared sufficient, without requirement to recruit monocytes from the bone marrow *via* CCR2.

There are at least two factors that could contribute to this finding: circulation and activation of Ly6C^{lo} monocytes could either be directly regulated by CCR2, or Ly6C^{lo} monocytes are derived from CCR2-dependent Ly6C^{hi} monocytes as their precursors. In support of the first mechanism, some studies show that there is low-grade expression of CCR2 on Ly6C^{lo} monocytes (44), which we also confirmed in our study. This low-grade expression of CCR2 could partially contribute to their exit

from the bone marrow. More importantly however, other studies support that Ly6C^{hi} monocytes are obligatory precursors of Ly6C^{lo} cells in blood and tissue (22, 26, 43, 61). It was shown that the transition of CCR2^{hi} CX3CR1^{lo} to CX3CR1^{hi} CCR2^{lo} monocytes in response to sterile injury is mediated by local production of the cytokines IL-4 and IL-10 (22). More specifically, Yona et al. demonstrated in a mixed bone marrow chimera that the generation of peripheral Ly6C^{lo} monocytes in steady state critically depends on CCR2-competent Ly6C^{hi} cells as their immediate precursors which require mobilization from the bone marrow (43). The observation that *CCR2*$^{-/-}$ mice harbor circulating Ly6C^{lo} monocytes (62) could, in fate-mapping mice, be explained by an extended lifespan of Ly6C^{lo} monocytes in the absence of Ly6C^{hi} monocytes (43). It is therefore likely that in *Orientia* infection, a large number Ly6C^{lo} monocytes differentiate from their CCR2-dependent Ly6C^{hi} precursor, resulting in an impaired response of both subsets in *CCR2*$^{-/-}$ mice. The delayed kinetics in induction of Ly6C^{lo} compared to Ly6C^{hi} responses in *Orientia* infection support that notion.

In sum, we provide here the first mechanistic study on blood and pulmonary monocyte/macrophage responses to *Orientia* in an i.d. mouse infection model. We established that both the extent and the activation of Ly6C^{hi} and Ly6C^{lo} monocyte responses depend on CCR2 in *Orientia* infection. The bacterial clearance from the lung, the development of interstitial pulmonary tissue lesions and the development of the inflammatory milieu were significantly delayed in the absence of CCR2. Correlating with these findings, CCR2 deficiency also delayed the development of clinical symptoms, suggesting an immunopathological role for inflammatory monocytes. We thus provide here a study that demonstrates a role for CCR2 in shaping systemic and pulmonary inflammation during *Orientia* infection.

DATA AVAILABILITY STATEMENT

The datasets generated for this study are available on request to the corresponding author.

ETHICS STATEMENT

The animal study was reviewed and approved by the Hamburg Authority for Health and Consumer Protection (no. 106/15).

AUTHOR CONTRIBUTIONS

MP: experimentation, data analysis, manuscript draft. CK: conceptualization and experimentation, data analysis, manuscript draft. MG: experimentation ZO: data analysis HL: conceptualization, material. BF: conceptualization, funding. JS: experimentation, data analysis. All authors contributed to the article and approved the submitted version.

FUNDING

CK received funding from the von Behring-Roentgen Foundation (grant 64-0011).

ACKNOWLEDGMENTS

We gratefully acknowledge the outstanding technical expertise of Ute Mehlhoop in maintaining *Orientia* culture and establishing the mRNA expression analysis. We also thank the Mouse Pathology Facility at UKE Hamburg, Germany (Prof. Dr. M. Glatzel, PD Dr. S. Krasemann, K. Hartmann) for providing immunohistological staining.

SUPPLEMENTARY MATERIAL

The Supplementary Material for this article can be found online at: https://www.frontiersin.org/articles/10.3389/fimmu.2021.670219/full#supplementary-material

REFERENCES

1. Paris DH, Phetsouvanh R, Tanganuchitcharnchai A, Jones M, Jenjaroen K, Vongsouvath M, et al. Orientia Tsutsugamushi in Human Scrub Typhus Eschars Shows Tropism for Dendritic Cells and Monocytes Rather Than Endothelium. *PLoS Negl Trop Dis* (2012) 6:e1466. doi: 10.1371/journal.pntd.0001466
2. Cho NH, Seong SY, Choi MS, Kim IS. Expression of Chemokine Genes in Human Dermal Microvascular Endothelial Cell Lines Infected With *Orientia Tsutsugamushi*. *Infect Immun* (2001) 69:1265–72. doi: 10.1128/IAI.69.3.1265-1272.2001
3. Cho NH, Seong SY, Huh MS, Han TH, Koh YS, Choi MS, et al. Expression of Chemokine Genes in Murine Macrophages Infected With *Orientia Tsutsugamushi*. *Infect Immun* (2000) 68:594–602. doi: 10.1128/IAI.68.2.594-602.2000
4. Cho NH, Seong SY, Huh MS, Kim NH, Choi MS, Kim IS. Induction of the Gene Encoding Macrophage Chemoattractant Protein 1 by *Orientia Tsutsugamushi* in Human Endothelial Cells Involves Activation of Transcription Factor Activator Protein 1. *Infect Immun* (2002) 70:4841–50. doi: 10.1128/IAI.70.9.4841-4850.2002
5. Ro HJ, Lee H, Park EC, Lee CS, Il Kim S, Jun S. Ultrastructural Visualization of *Orientia Tsutsugamushi* in Biopsied Eschars and Monocytes From Scrub Typhus Patients in South Korea. *Sci Rep* (2018) 8:17373. doi: 10.1038/s41598-018-35775-9
6. Walsh DS, Myint KS, Kantipong P, Jongsakul K, Watt G. *Orientia Tsutsugamushi* in Peripheral White Blood Cells of Patients With Acute Scrub Typhus. *Am J Trop Med Hyg* (2001) 65:899–901. doi: 10.4269/ajtmh.2001.65.899
7. Keller CA, Hauptmann M, Kolbaum J, Gharaibeh M, Neumann M, Glatzel M, et al. Dissemination of *Orientia Tsutsugamushi* and Inflammatory Responses in a Murine Model of Scrub Typhus. *PLoS Negl Trop Dis* (2014) 8:e3064. doi: 10.1371/journal.pntd.0003064
8. Trent B, Liang Y, Xing Y, Esqueda M, Wei Y, Cho NH, et al. Polarized Lung Inflammation and Tie2/Angiopoietin-Mediated Endothelial Dysfunction During Severe *Orientia Tsutsugamushi* Infection. *PLoS Negl Trop Dis* (2020) 14:1–22. doi: 10.1371/journal.pntd.0007675
9. Rikihisa Y, Ito S. Intracellular Localization of Rickettsia Tsutsugamushi in Polymorphonuclear Leukocytes. *J Exp Med* (1979) 150(3):703–8. doi: 10.1084/jem.150.3.703
10. Tantibhedhyangkul W, Prachason T, Waywa D, El Filali A, Ghigo E, Thongnoppakhun W, et al. *Orientia Tsutsugamushi* Stimulates an Original

Gene Expression Program in Monocytes: Relationship With Gene Expression in Patients With Scrub Typhus. *PLoS Negl Trop Dis* (2011) 5:e1028. doi: 10.1371/journal.pntd.0001028
11. Astrup E, Janardhanan J, Otterdal K, Ueland T, Prakash JAJ, Lekva T, et al. Cytokine Network in Scrub Typhus: High Levels of Interleukin-8 Are Associated With Disease Severity and Mortality. *PLoS Negl Trop Dis* (2014) 8:1–9. doi: 10.1371/journal.pntd.0002648
12. Boring L, Gosling J, Cleary M, Charo IF. Decreased Lesion Formation in CCR2(-/-) Mice Reveals a Role for Chemokines in the Initiation of Atherosclerosis. *Nature* (1998) 394:894–7. doi: 10.1038/29788
13. Kurihara T, Warr G, Loy J, Bravo R. Defects in Macrophage Recruitment and Host Defense in Mice Lacking the CCR2 Chemokine Receptor. *J Exp Med* (1997) 186:1757–62. doi: 10.1084/jem.186.10.1757
14. Serbina NV, Pamer EG. Monocyte Emigration From Bone Marrow During Bacterial Infection Requires Signals Mediated by Chemokine Receptor CCR2. *Nat Immunol* (2006) 7:311–7. doi: 10.1038/ni1309
15. Peters W, Scott HM, Chambers HF, Flynn JL, Charo IF, Ernst JD. Chemokine Receptor 2 Serves an Early and Essential Role in Resistance to *Mycobacterium Tuberculosis*. *Proc Natl Acad Sci* (2001) 98:7958–63. doi: 10.1073/pnas.131207398
16. Lim JK, Obara CJ, Rivollier A, Pletnev AG, Kelsall BL, Murphy PM. Chemokine Receptor Ccr2 Is Critical for Monocyte Accumulation and Survival in West Nile Virus Encephalitis. *J Immunol* (2011) 186:471–8. doi: 10.4049/jimmunol.1003003
17. Biswas A, Bruder D, Wolf SA, Jeron A, Mack M, Heimesaat MM, et al. Ly6C High Monocytes Control Cerebral Toxoplasmosis. *J Immunol* (2015) 194:3223–35. doi: 10.4049/jimmunol.1402037
18. Helk E, Bernin H, Ernst T, Ittrich H, Jacobs T, Heeren J, et al. TNFα-Mediated Liver Destruction by Kupffer Cells and Ly6Chi Monocytes During *Entamoeba Histolytica* Infection. *PLoS Pathog* (2013) 9:e1003096. doi: 10.1371/journal.ppat.1003096
19. Shi C, Pamer EG. Monocyte Recruitment During Infection and Inflammation. *Nat Rev Immunol* (2011) 11:762–74. doi: 10.1038/nri3070
20. Auffray C, Fogg D, Garfa M, Elain G, Join-Lambert O, Kayal S, et al. Monitoring of Blood Vessels and Tissues by a Population of Monocytes With Patrolling Behavior. *Science (80-)* (2007) 317:666–70. doi: 10.1126/science.1142883
21. Rahman K, Vengrenyuk Y, Ramsey SA, Vila NR, Girgis NM, Liu J, et al. Inflammatory Ly6Chi Monocytes and Their Conversion to M2 Macrophages Drive Atherosclerosis Regression. *J Clin Invest* (2017) 127:2904–15. doi: 10.1172/JCI75005
22. Dal-Secco D, Wang J, Zeng Z, Kolaczkowska E, Wong CHY, Petri B, et al. A Dynamic Spectrum of Monocytes Arising From the *In Situ* Reprogramming of CCR2+ Monocytes at a Site of Sterile Injury. *J Exp Med* (2015) 212:447–56. doi: 10.1084/jem.20141539
23. Ginhoux F, Greter M, Leboeuf M, Nandi S, See P, Gokhan S, et al. Fate Mapping Analysis Reveals That Adult Microglia Derive From Primitive Macrophages. *Science* (2014) 330(6005):841–5. doi: 10.1126/science.1194637
24. Gomez Perdiguero E, Klapproth K, Schulz C, Busch K, Azzoni E, Crozet L, et al. Tissue-Resident Macrophages Originate From Yolk-Sac-Derived Erythro-Myeloid Progenitors. *Nature* (2015) 518:547–51. doi: 10.1038/nature13989
25. Scott CL, Zheng F, De Baetselier P, Martens L, Saeys Y, De Prijck S, et al. Bone Marrow-Derived Monocytes Give Rise to Self-Renewing and Fully Differentiated Kupffer Cells. *Nat Commun* (2016) 7:1–10. doi: 10.1038/ncomms10321
26. Hilgendorf I, Gerhardt LMS, Tan TC, Winter C, Holderried TAW, Chousterman BG, et al. Ly-6 Chigh Monocytes Depend on Nr4a1 to Balance Both Inflammatory and Reparative Phases in the Infarcted Myocardium. *Circ Res* (2014) 114:1611–22. doi: 10.1161/CIRCRESAHA.114.303204
27. Mackaness GB. Cellular Resistance to Infection. *J Exp Med* (1962) 116:381–406. doi: 10.1084/jem.116.3.381
28. Nathan CF, Murray HW, Wlebe IE, Rubin BY. Identification of Interferon-γ, as the Lymphokine That Activates Human Macrophage Oxidative Metabolism and Antimicrobial Activity. *J Exp Med* (1983) 158:670–89. doi: 10.1084/jem.158.3.670
29. Stein M, Keshav S, Harris N, Gordon S. Interleukin 4 Potently Enhances Murine Macrophage Mannose Receptor Activity: A Marker of Alternative Immunologic Macrophage Activation. *J Exp Med* (1992) 176:287–92. doi: 10.1084/jem.176.1.287
30. Mills CD, Kincaid K, Alt JM, Heilman MJ, Hill AM. M-1/M-2 Macrophages and the Th1/Th2 Paradigm. *J Immunol* (2000) 164:6166–73. doi: 10.4049/jimmunol.164.12.6166
31. Murray PJ, Allen JE, Biswas SK, Fisher EA, Gilroy DW, Goerdt S, et al. Macrophage Activation and Polarization: Nomenclature and Experimental Guidelines. *Immunity* (2014) 41:14–20. doi: 10.1016/j.immuni.2014.06.008
32. Martinez FO, Gordon S. The M1 and M2 Paradigm of Macrophage Activation: Time for Reassessment. *F1000Prime Rep* (2014) 6:1–13. doi: 10.12703/P6-13
33. Shi C, Jia T, Mendez-Ferrer S, Hohl TM, Serbina NV, Lipuma L, et al. Bone Marrow Mesenchymal Stem and Progenitor Cells Induce Monocyte Emigration in Response to Circulating Toll-Like Receptor Ligands. *Immunity* (2011) 34:590–601. doi: 10.1016/j.immuni.2011.02.016
34. Chen HC, Chang HC, Chang YC, Liu SF, Su MC, Huang KT, et al. Chest Radiographic Presentation in Patients With Scrub Typhus. *Trans R Soc Trop Med Hyg* (2012) 106:48–53. doi: 10.1016/j.trstmh.2011.09.005
35. Song SW, Kim KT, Ku YM, Park SH, Kim YS, Lee DG, et al. Clinical Role of Interstitial Pneumonia in Patients With Scrub Typhus: A Possible Marker of Disease Severity. *J Korean Med Sci* (2004) 19:668–73. doi: 10.3346/jkms.2004.19.5.668
36. Jeong YJ, Kim S, Wook YD, Lee JW, Kim K-I, Lee SH. Scrub Typhus: Clinical, Pathologic, and Imaging Findings. *Radiographics* (2007) 27:161–72. doi: 10.1148/rg.271065074
37. Boring L, Gosling J, Chensue SW, Kunkel SL, Farese RV, Broxmeyer HE, et al. Impaired Monocyte Migration and Reduced Type 1 (Th1) Cytokine Responses in C-C Chemokine Receptor 2 Knockout Mice. *J Clin Invest* (1997) 100(10):2552–61. doi: 10.1172/JCI119798
38. Kuziel WA, Morgan SJ, Dawson TC, Griffin S, Smithies O, Ley K, et al. Severe Reduction in Leukocyte Adhesion and Monocyte Extravasation in Mice Deficient in CC Chemokine Receptor 2. *Proc Natl Acad Sci USA* (1997) 94:12053–8. doi: 10.1073/pnas.94.22.12053
39. Sellau J, Groneberg M, Fehling H, Thye T, Hoenow S, Marggraff C, et al. Androgens Predispose Males to Monocyte-Mediated Immunopathology by Inducing the Expression of Leukocyte Recruitment Factor CXCL1. *Nat Commun* (2020) 11(1):3459. doi: 10.1038/s41467-020-17260-y
40. Cole LE, Elkins KL, Michalek SM, Qureshi N, Eaton LJ, Rallabhandi P, et al. Immunologic Consequences of Francisella Tularensis Live Vaccine Strain Infection: Role of the Innate Immune Response in Infection and Immunity. *J Immunol* (2006) 176:6888–99. doi: 10.4049/jimmunol.176.11.6888
41. Sasaki Y, Ohsawa K, Kanazawa H, Kohsaka S, Imai Y. Iba1 Is an Actin-Cross-Linking Protein in Macrophages/Microglia. *Biochem Biophys Res Commun* (2001) 286:292–7. doi: 10.1006/bbrc.2001.5388
42. Hauptmann M, Kolbaum J, Lilla S, Wozniak D, Gharaibeh M, Fleischer B, et al. Protective and Pathogenic Roles of CD8+ T Lymphocytes in Murine *Orientia Tsutsugamushi* Infection. *PLoS Negl Trop Dis* (2016) 10:e0004991. doi: 10.1371/journal.pntd.0004991
43. Yona S, Kim KW, Wolf Y, Mildner A, Varol D, Breker M, et al. Fate Mapping Reveals Origins and Dynamics of Monocytes and Tissue Macrophages Under Homeostasis. *Immunity* (2013) 38:79–91. doi: 10.1016/j.immuni.2012.12.001
44. Schmid MA, Harris E. Monocyte Recruitment to the Dermis and Differentiation to Dendritic Cells Increases the Targets for Dengue Virus Replication. *PLoS Pathog* (2014) 10:e1004541. doi: 10.1371/journal.ppat.1004541
45. Swirski FK, Nahrendorf M, Etzrodt M, Wildgruber M, Cortez-Retamozo V, Panizzi P, et al. Identification of Splenic Reservoir Monocytes and Their Deployment to Inflammatory Sites. *Science (80-)* (2009) 325:612–6. doi: 10.1126/science.1175202
46. Hettinger J, Richards DM, Hansson J, Barra MM, Joschko AC, Krijgsveld J, et al. Origin of Monocytes and Macrophages in a Committed Progenitor. *Nat Immunol* (2013) 14:821–30. doi: 10.1038/ni.2638
47. Geissmann F, Jung S, Littman DR. Blood Monocytes Consist of Two Principal Subsets With Distinct Migratory Properties. *Immunity* (2003) 19:71–82. doi: 10.1016/S1074-7613(03)00174-2
48. Drevets DA, Dillon MJ, Schawang JS, Van Rooijen N, Ehrchen J, Sunderkötter C, et al. The Ly-6Chigh Monocyte Subpopulation Transports *Listeria*

Monocytogenes Into the Brain During Systemic Infection of Mice. *J Immunol* (2004) 172:4418–24. doi: 10.4049/jimmunol.172.7.4418
49. Courret N, Darche S, Sonigo P, Milon G, Buzoni-Gâtel D, Tardieux I. CD11c- and CD11b-Expressing Mouse Leukocytes Transport Single *Toxoplasma Gondii* Tachyzoites to the Brain. *Blood* (2006) 107:309–16. doi: 10.1182/blood-2005-02-0666
50. Liu PJ, Chen YS, Lin HH, Ni WF, Hsieh TH, Chen HT, et al. Induction of Mouse Melioidosis With Meningitis by CD11b+ Phagocytic Cells Harboring Intracellular *B. Pseudomallei* as a Trojan Horse. *PLoS Negl Trop Dis* (2013) 7: e2363. doi: 10.1371/journal.pntd.0002363
51. Menasria R, Canivet C, Piret J, Gosselin J, Boivin G. Both Cerebral and Hematopoietic Deficiencies in CCR2 Result in Uncontrolled Herpes Simplex Virus Infection of the Central Nervous System in Mice. *PLoS One* (2016) 11: e0168034. doi: 10.1371/journal.pone.0168034
52. Szymczak WA, Deepe GS Jr. The CCL7-CCL2-CCR2 Axis Regulates IL-4 Production in Lungs and Fungal Immunity. *J Immunol* (2009) 183:1964–74. doi: 10.4049/jimmunol.0901316
53. Dunay IR, Fuchs A, Sibley LD. Inflammatory Monocytes But Not Neutrophils Are Necessary To Control Infection With *Toxoplasma Gondii* in Mice. *Infect Immun* (2010) 78:1564–70. doi: 10.1128/IAI.00472-09
54. Benevides L, Milanezi CM, Yamauchi LM, Benjamim CF, Silva JS, Silva NM. CCR2 Receptor Is Essential to Activate Microbicidal Mechanisms to Control *Toxoplasma Gondii* Infection in the Central Nervous System. *Am J Pathol* (2008) 173:741–51. doi: 10.2353/ajpath.2008.080129
55. Kay E, Gomez-Garcia L, Woodfin A, Scotland RS, Whiteford JR. Sexual Dimorphisms in Leukocyte Trafficking in a Mouse Peritonitis Model. *J Leukoc Biol* (2015) 98:805–17. doi: 10.1189/jlb.3A1214-601RR
56. Jenkins SJ, Ruckerl D, Cook PC, Jones LH, Finkelman FD, van Rooijen N, et al. Local Macrophage Proliferation, Rather Than Recruitment From the Blood, Is a Signature of TH2 Inflammation. *Science* (2011) 332:1284–8. doi: 10.1126/science.1204351
57. Soong L, Wang H, Shelite TR, Liang Y, Mendell NL, Sun J, et al. Strong Type 1, But Impaired Type 2, Immune Responses Contribute to *Orientia Tsutsugamushi*-Induced Pathology in Mice. *PLoS Negl Trop Dis* (2014) 8(9): e3191. doi: 10.1371/journal.pntd.0003191
58. Soong L, Mendell NL, Olano JP, Rockx-Brouwer D, Xu G, Goez-Rivillas Y, et al. An Intradermal Inoculation Mouse Model for Immunological Investigations of Acute Scrub Typhus and Persistent Infection. *PLoS Negl Trop Dis* (2016) 10:e0004884. doi: 10.1371/journal.pntd.0004884
59. Traynor TR, Kuziel WA, Toews GB, Huffnagle GB. CCR2 Expression Determines T1 Versus T2 Polarization During Pulmonary *Cryptococcus Neoformans* Infection. *J Immunol* (2000) 164:2021–7. doi: 10.4049/jimmunol.164.4.2021
60. Hammond MD, Taylor RA, Mullen MT, Ai Y, Aguila HL, Mack M, et al. CCR2+Ly6Chi Inflammatory Monocyte Recruitment Exacerbates Acute Disability Following Intracerebral Hemorrhage. *J Neurosci* (2014) 34:3901–9. doi: 10.1523/JNEUROSCI.4070-13.2014
61. Varga T, Mounier R, Gogolak P, Poliska S, Chazaud B, Nagy L. Tissue LyC6 – Macrophages Are Generated in the Absence of Circulating LyC6 – Monocytes and Nur77 in a Model of Muscle Regeneration. *J Immunol* (2013) 191:5695–701. doi: 10.4049/jimmunol.1301445
62. Qu C, Edwards EW, Tacke F, Angeli V, Llodrá J, Sanchez-Schmitz G, et al. Role of CCR8 and Other Chemokine Pathways in the Migration of Monocyte-Derived Dendritic Cells to Lymph Nodes. *J Exp Med* (2004) 200:1231–41. doi: 10.1084/jem.20032152

Conflict of Interest: The authors declare that the research was conducted in the absence of any commercial or financial relationships that could be construed as a potential conflict of interest.

Supplementary figures

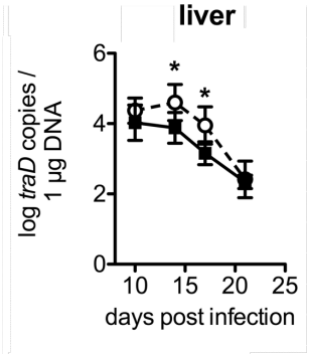

Fig. S1 Delayed clearance of *O. tsutsugamushi* in liver tissue of *CCR2*$^{-/-}$ mice

CCR2$^{-/-}$ or C57BL/6 mice were infected with 5,000 sfu *O. tsutsugamushi* in the hind footpad. Per genotype, n=3 mice were sacrificed on days 10, 14, 17 and 21, and bacterial concentrations were quantified from the liver by *traD*-specific qPCR. Data from two independent experiments were pooled; shown are means of bacterial concentrations from organs of n=2x3=6 mice per genotype and time point ± SD. * $p<0.05$ by two-way ANOVA.

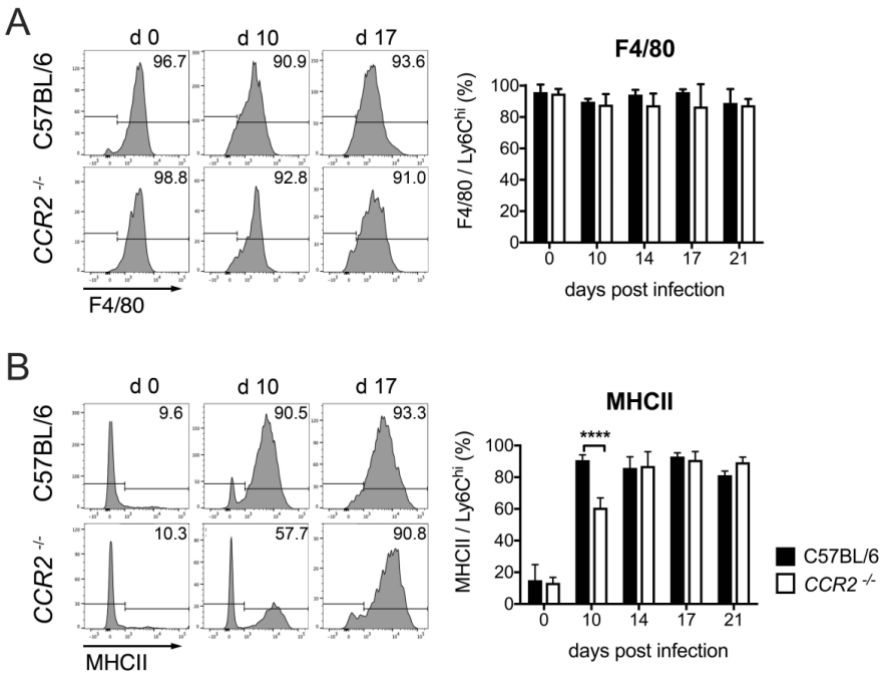

Fig. S2 Expression of MHCII but not F4/80 on *CCR2*$^{-/-}$ Ly6C^{hi} pulmonary monocytes is delayed during infection with *O. tsutsugamushi*

On CD11b^{+} Ly6C^{hi} pulmonary monocytes from infected C57BL/6 and *CCR2*$^{-/-}$ mice, the expression of F4/80 (A) and MHCII (B) was measured by FACS. Shown are percentages of positive Ly6C^{hi} cells expressing the respective marker (histograms and statistics). Data were pooled from 2 independent experiments (n=2x3=6 mice per timepoint and genotype, mean ± SD). * p<0.05; ** p<0.01; *** p<0.001 by two way-ANOVA.

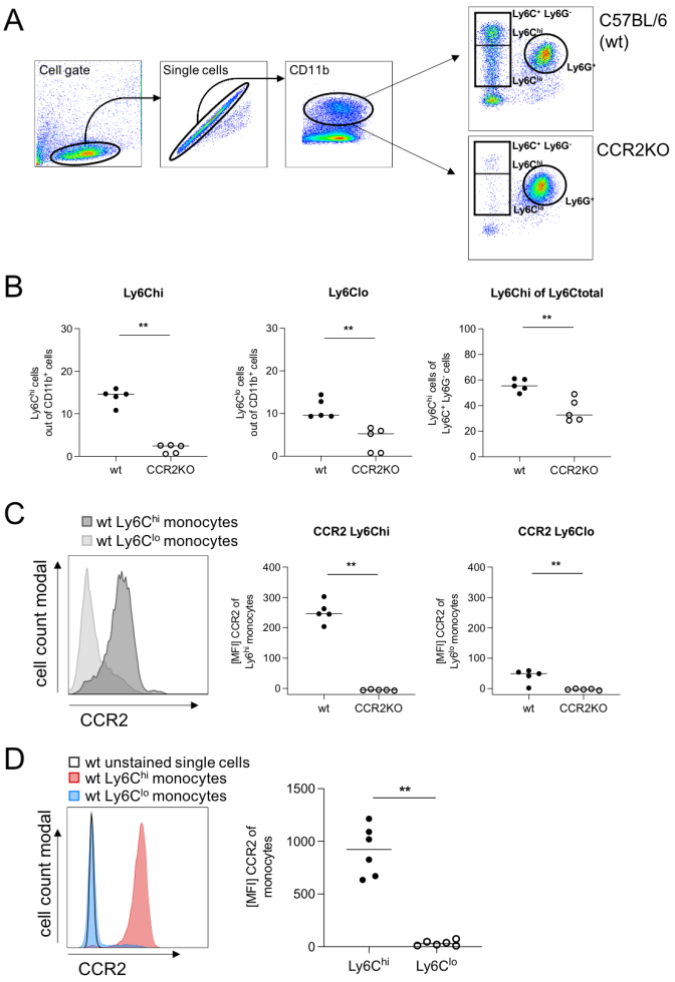

Fig. S3 Expression of CCR2 on CD11b^{+} Ly6C^{hi} and Ly6C^{lo} monocytes

PBMC from peripheral blood of C57BL/6 and *CCR2*$^{-/-}$ mice were stained for CD11b, Ly6C, Ly6 and CCR2 (n=5 animals). (A) Gating strategy. (B) Among all CD11b^{+} cells, C57BL/6 mice show higher percentages of Ly6C^{hi} and Ly6C^{lo} monocytes than *CCR2*$^{-/-}$ mice (left and middle panel), and higher percentages of Ly6C^{hi} per all Ly6C^{+} monocytes (right panel). (C) CCR2 expression on Ly6C^{hi} and Ly6C^{lo} monocytes (histogram for C57BL/6 mice, left panel). C57BL/6 express higher levels of CCR2 than *CCR2*$^{-/-}$ mice not only in Ly6C^{hi} (middle panel) but also Ly6C^{lo} monocytes (right panel). (D) Histogram of CCR2 staining with unstained control. **, p<0.01 by Mann-Whitney test.

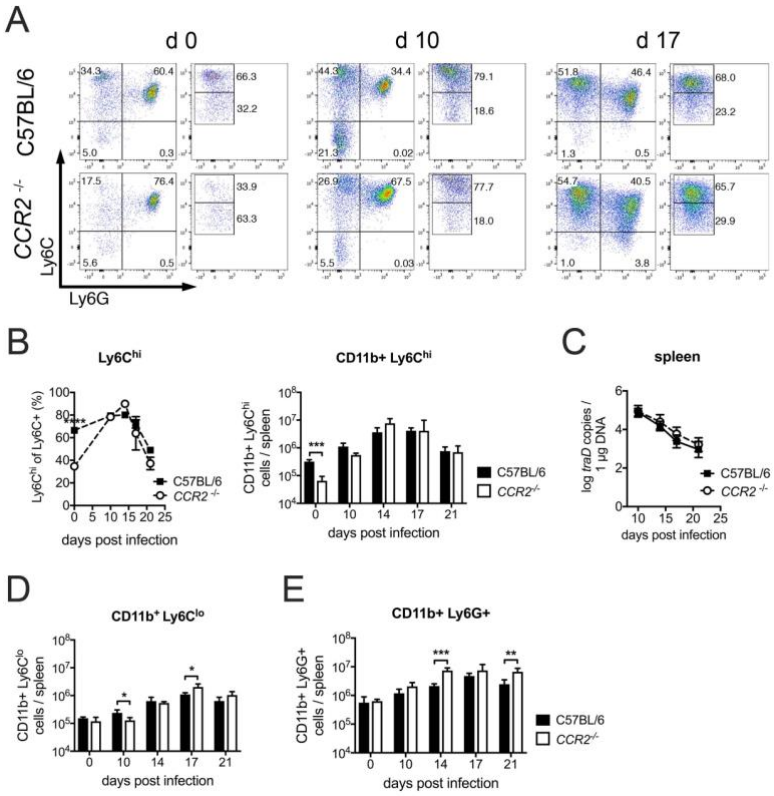

Fig. S4 CCR2 deficiency does not cause profound deficits in splenic monocyte/neutrophil responses and antibacterial defense during infection with *O. tsutsugamushi*

C57BL/6 and *CCR2*$^{-/-}$ mice were infected with 5,000 sfu *O. tsutsugamushi* in the hind footpad, and spleens were removed at days 10, 14, 17 and 21 p.i. and processed for further analysis. (A) Expression of Ly6C and Ly6G was measured by FACS on pre-gated CD11b^{+} cells (see Fig. 3). (B) Shown are percentages of positive Ly6C^{hi} of all LyC+ cells (left panel) and the entire number of CD11b^{+} Ly6C^{hi} cells per spleen (right panel). (C) On days 10, 14, 17 and 21 p.i., the bacterial concentration was measured by *traD* qPCR from spleen samples. (D) The size of CD11b^{+} Ly6C^{lo} monocyte and (E) CD11b^{+} Ly6G^{+} granulocyte populations was analyzed from FACS data. Data in C were from two independent experiments (n=6 mice per genotype and timepoint, mean ± SD); data in A,B,D,E were from one experiment (n=3 mice per genotype and timepoint, mean ± SD). * p<0.05; ** p<0.01; *** p<0.001, **** p<0.0001 by two way-ANOVA.

2. Darstellung der Publikation mit Literaturverzeichnis

2.1 *Orientia tsutsugamushi*

Orientia (O.) tsutsugamushi, ein Gram-negatives und obligat intrazelluläres Bakterium, ist der Auslöser des Tsutsugamushi-Fiebers (englisch: scrub typhus). Die Erkrankung betrifft vornehmlich den ostasiatischen Pazifikraum im sogenannten Tsutsugamushi-Dreieck, Infektionen in Afrika und Südamerika sind beschrieben (Jiang, Richards 2018). Die Übertragung von *O. tsutsugamushi* erfolgt über die Haut während des Bisses infektiöser Milbenlarven als Vektoren. Nach einer Infektion kommt es an der Inokulationsstelle zu einer Hautnekrose, welche in leichten Verläufen von Fieber und grippeartigen Symptomen begleitet wird (Paris, Phetsouvanh et al. 2012). In schwereren Fällen sind interstitielle Lungenentzündungen und akutes Lungenversagen bis zum Multiorganversagen beschrieben (Chi, Huang et al. 1997, Astrup, Janardhanan et al. 2014). Unbehandelt kann das Tsutsugamushifieber letal verlaufen. Pro Jahr betrifft die Erkrankung nach Schätzung der Weltgesundheitsorganisation (WHO) etwa 1 Million Menschen (Kelly, Fuerst et al. 2009). Eine antibiotische Behandlung mit Doxycyclin (Wangrangsimakul, Phuklia et al. 2020), alternativ Rifampicin oder Makroliden (Luce-Fedrow, Lehman et al. 2018) ist effektiv. Im Mausmodell lässt sich eine deutliche Makrophagenantwort und ein Tropismus des Erregers für Monozyten und Makrophagen sowie eine Lungenbeteiligung mit interstitiellen und peribronchialen Makrophagenläsionen feststellen (Keller, Hauptmann et al. 2014). Auch in der Lunge menschlicher Patienten ist eine interstitielle Lungenentzündung typisch (Song, Kim et al. 2004, Jeong, Kim et al. 2007, Chen, Chang et al. 2012). In der vorliegenden Arbeit wurde zur Untersuchung der Rolle von Monozyten ein selbstheilendes Mausmodell in der C57BL/6-Maus gewählt. Die am Fuß intradermal durchgeführte Infektion der Tiere kommt dem natürlichen Infektionsweg sehr nahe (Hauptmann, Kolbaum et al. 2016). Verwendet wurde der humanpathogene Karp-Stamm des Bakteriums, welcher sich in BALB/c-Mäusen im Gegensatz zum Gilliam-Stamm bei einer intraperitonealen Infektion als letal erweist (Groves, Kelly 1989).

2.2 Monozyten und Makrophagen als Teil der Immunantwort

Einen wichtigen Teil der Immunantwort auf die Infektion mit *O. tsutsugamushi* stellt bei Menschen und Mäusen eine Induktion Monozyten-bezogener Chemokine dar (Cho, Seong et al. 2000, Cho, Seong et al. 2001, Cho, Seong et al. 2002, Luce-Fedrow, Lehman et al. 2018).

Monozyten gehören zum mononukleären Phagozytensystem (MPS). Sie finden sich im Blut, Knochenmark und der Milz und entwickeln sich aus einer sequentiellen Reihe hämatopoetischer Stammzellen im Knochenmark. In Mäusen werden zwei verschiedene Monozytentypen unterschieden (Italiani, Boraschi 2014). Zum einen sind dies inflammatorische Monozyten, identifiziert anhand der Oberflächenmarker $CD11b^{+}$, $Ly6C^{hi}$, $Ly6G^{-}$. Sie werden zügig zu Infektions- oder Entzündungsherden rekrutiert (Serbina, Jia et al. 2008). Von ihnen wird außerdem der CC Chemokinrezeptor 2 (CCR2), ein Rezeptor für die Chemokine CC-chemokine ligand 2 und 7

(CCL2/CCL7), stark exprimiert (Shi, Pamer 2011). Für den Austritt der Ly6C^{hi}-Monozyten aus dem Knochenmark ist die Bindung von CCL2 an CCR2 entscheidend. Shi et al. wiesen nach, dass hierfür eine lokale Produktion von CCL2 im Knochenmark erforderlich ist: Mesenchymale Stammzellen produzieren CCL2 als Reaktion auf geringe Mengen zirkulierender Toll-like-Rezeptor (TLR)-Liganden und lösen damit die Freisetzung von Ly6C^{hi}/CCR2^{+}-Monozyten in die Blutbahn aus (Shi, Jia et al. 2011). Neben der Aktivierung von Toll-like-Rezeptoren scheinen auch Typ I-Interferone einen Einfluss auf die CCL2-Produktion zu haben (Serbina, Shi et al. 2012). So beeinflussen CCR2-vermittelte Signale im Knochenmark die Häufigkeit von Ly6C^{hi}-Monozyten im Blutkreislauf (Serbina, Pamer 2006). Dieser Monozytentyp wird also aus dem Knochenmark zum jeweiligen Inflammationsherd rekrutiert (Shi, Pamer 2011). Zum einen scheint dieser Zelltyp unter steady-state-Bedingungen bestimmte „Makrophagendepots“ u.a. im Verdauungstrakt (Rivollier, He et al. 2012), in der Haut (Tamoutounour, Guilliams et al. 2013), im Herzen (Epelman, Lavine et al. 2014) und in der Lunge (Guilliams, De Kleer et al. 2013) auszutauschen und zu ersetzen, zum anderen infiltrieren diese Monozyten erkranktes Gewebe in großer Anzahl und differenzieren zu inflammatorischen Makrophagen oder Tip-DC´s (TNF/iNOS-Producing Dendritic Cells) (Serbina, Salazar-Mather et al. 2003). Bei Mäusen, die CCR2 nicht exprimieren, ist die CCR2-abhängige Rekrutierung inflammatorischer Ly6C^{hi}-Zellen aus dem Knochenmark gestört. Es werden schwere Defizite bei der Rekrutierung inflammatorischer Monozyten und Gewebemakrophagen zum Beispiel unter einer Infektion mit *Listeria monocytogenes* oder bei der Bildung arteriosklerotischer Plaques beobachtet (Kurihara, Warr et al. 1997, Boring, Gosling et al. 1998, Serbina, Pamer 2006). Folglich kann eine Infektion bei von einem CCR2-Mangel betroffenen Mäusen mit einem protrahierten Krankheitsverlauf einhergehen, zum Beispiel bei Infektionen mit *Listeria monocytogenes*, *Mycobacterium tuberculosis* oder *Toxoplasma gondii* (Kurihara, Warr et al. 1997, Peters, Scott et al. 2001, Italiani, Boraschi 2014, Biswas, Bruder et al. 2015). Andererseits kann die Abwesenheit dieser inflammatorischen Monozyten einen Infektionsverlauf auch günstig modulieren, zum Beispiel bei Amöbiasis (Helk, Bernin et al. 2013), oder zu einem milderen Krankheitsbild führen, beispielsweise bei Arteriosklerose (Boring, Gosling et al. 1998). Neben diesen inflammatorischen Monozyten existieren residente Monozyten, klassifiziert als CD11b^{+} Ly6C^{lo} Ly6G^{-}. Diese Zellen exprimieren hohe Level von CX_3CR_1-Rezeptoren, jedoch nur geringe CCR2-Level und sind somit von einer CCR2-vermittelten Rekrutierung aus dem Knochenmark nicht unmittelbar betroffen (Shi, Pamer 2011). Dieser Zelltyp ist durch patrouillierende Funktionen im und am Gefäßendothel charakterisiert (Auffray, Fogg et al. 2007). Von hier aus können diese Zellen in entzündetes Gewebe einwandern, und dann beispielsweise nach Differenzierung in Makrophagen unter Hochregulation der Transkriptionsfaktoren cMaf und Mafb regenerierende Funktionen („tissue repair“) übernehmen (Auffray, Fogg et al. 2007, Nahrendorf, Swirski et al. 2007). cMaf und Mafb als Transkriptionsfaktoren unterstützen dabei eine M2-Polarisierung (siehe unten) von Makrophagen (Kim 2017, Liu, Tong et al. 2020).

Makrophagen werden ebenfalls dem mononukleären Phagozytensystem zugerechnet. Es handelt sich um einen sehr heterogenen Zelltyp, der je nach Gewebe hochspezialisiert ist und entsprechend benannt wird (z.B. Osteoklasten, Alveolarmakrophagen, Langerhanszellen, Kupfferzellen) (Gautier, Shay et al. 2012). Gemeinsam ist ihnen die Aufgabe der Aufrechterhaltung der Homöostase innerhalb der verschiedenen Gewebe, („remodelling and tissue repair“) und die Immunabwehr mittels Phagozytose, Antigenpräsentation, Sekretion von Chemokinen, pro- und antiinflammatorischen Zytokinen oder auch Wachstumsfaktoren. In der Durchflusszytometrie lassen sie sich neben den bereits für die Monozyten erwähnten Oberflächenmarkern auch durch das Oberflächenmolekül F4/80 identifizieren (Gordon, Hamann et al. 2011), histologisch lassen sie sich über eine IBA1 (ionized calcium binding adapter molecule 1)-Färbung darstellen (Sasaki, Ohsawa et al. 2001). Die Vorstellung, dass Gewebsmakrophagen unter steady-state-Bedingungen ausschließlich von zirkulierenden Monozyten aus dem Blut stammen, gilt mittlerweile als weitgehend überholt. Zum einen konnte gezeigt werden, dass embryonale Vorläuferzellen aus dem Dottersack existieren, von denen Makrophagen abstammen (Epelman, Lavine et al. 2014, Gomez Perdiguero, Klapproth et al. 2015), zum anderen ist bekannt, dass Gewebsmakrophagen ihren Bestand mittels lokaler Proliferation aufrecht erhalten können (Hashimoto, Chow et al. 2013, Ginhoux, Jung 2014). Im Blut zirkulierende, aus dem Knochenmark stammende Monozyten können aber residente Makrophagenpopulationen durch Infiltration ersetzen (Scott, Zheng et al. 2016). Es zeigt sich hier also ein weiterer Hinweis für die große Plastizität und Flexibilität innerhalb des Monozyten-Makrophagensystems. Die aktivierten Phänotypen von Makrophagen werden von einigen Autoren in ein veranschaulichendes M1/M2-Konzept eingeteilt. Während M1-Makrophagen hauptsächlich eine entzündungsfördernde Funktion zugesprochen wird, sollen M2-Makrophagen an entzündungshemmenden bzw. regenerierenden Reaktionen beteiligt sein (Mills 2012, Yunna, Mengru et al. 2020). Die Funktion der unterschiedlichen Aktivierung der Makrophagensubtypen beruht auf einem unterschiedlichen Arginin-Stoffwechsel. M1-Makrophagen exprimieren Stickoxid (NO)-Synthase, das Arginin zu NO und Citrullin metabolisiert. M2-Makrophagen exprimieren das Enzyms Arginase, das Arginin zu Ornithin und Harnstoff hydrolysiert (Rath, Müller et al. 2014). Ornithin wirkt unterstützend im Rahmen der Gewebeheilung und Zellproliferation, im Gegensatz dazu ist NO ein wirkungsvolles Bakterizid (MacMicking, Xie et al. 1997). *In vitro* lässt sich eine Polarisation der Makrophagen in Richtung des M1-Phänotyps durch infektiöse Mikroorganismen oder zum Beispiel durch Lipopolysaccharid, Tumornekrosefaktor (TNF)-α oder Interferon (IFN)-γ stimulieren. M1-Makrophagen produzieren neben toxischem NO und reaktiven Sauerstoffspezies wie Superoxidanionen auch inflammatorische Zytokine wie IL-1β, TNF, IL-6 und induzieren eine Th1-Polarisation von $CD4^+$-Zellen (Italiani, Boraschi 2014). Die M2-Polarisation von Makrophagen gilt als das „Standard-Programm“ geweberesidenter Makrophagen (Murray, Wynn 2011). Sie kann *in vitro* durch Th2-assoziierte Chemokine wie IL-4 und IL-13, bestimmte TLR-Liganden und antiinflammatorische Moleküle wie IL-10, Transforming-Growth-Factor (TGF)-β sowie

Glukokortikoide forciert werden (Martinez, Sica et al. 2008, Gordon, Martinez 2010). M2-aktivierte Makrophagen verstärken die Th2-Polarisation, „tissue remodelling“, allergische Reaktionen und Angiogenese (Sica, Mantovani 2012). Allerdings konnte am Beispiel der Multiplen Sklerose gezeigt werden, dass einzelne Makrophagen auch gemischte Phänotypen aufzeigen können (Vogel, Vereyken et al. 2013). Die zunehmende Identifizierung vieler weiterer polarisierender Stimuli und neuer Sub-Phänotypen der Polarisation zeigt die Limitation des M1/M2-Konzeptes (Martinez, Gordon 2014). Eine weitere Frage ist, ob und wie eine phänotypische und funktionelle Differenzierung von Makrophagen auch *in vivo* stattfindet. Hierzu gibt es mehrere Hypothesen, die kontrovers diskutiert werden (Italiani, Boraschi 2014). Es konnte aber sowohl die Differenzierung von Ly6C^{hi}-Zellen in M1-Makrophagen und von Ly6C^{lo}-Zellen in M2-Makrophagen (Auffray, Fogg et al. 2007, Nahrendorf, Swirski et al. 2007) als auch die Differenzierung von Ly6C^{hi}-M1-Zellen zu Ly6C^{lo}-M2-Zellen beobachtet werden (Crane, Daley et al. 2014). Während gezeigt wurde, dass *O. tsutsugamushi* die M1-Reaktionen in der Lunge induziert (Trent, Liang et al. 2020), wurden bisher keine Studien zur Chemokin-gesteuerten Rekrutierung myeloischer Zellen in der Infektion mit *O. tsutsugamushi* veröffentlicht. Allerdings sind erhöhte Plasmakonzentrationen der Chemokine CC-Chemokine Liganden 2 und 4 (CCL2/CCL4, monocyte chemoattractant protein-1/macrophage inflammatory protein-1b) bei schweren Verläufen einer Infektion mit *O. tsutsugamushi* beschrieben (Astrup, Janardhanan et al. 2014). In der vorliegenden Arbeit wurde die Hypothese aufgestellt, dass CCR2 für die Entwicklung pulmonaler Monozyten-/Makrophagen-Reaktionen und die damit verbundene bakterielle Clearance bei *O. tsutsugamushi*-Infektionen entscheidend ist. In einem Modell der intradermalen *O. tsutsugamushi*-Mausinfektion konnte eine relevante Rolle von CCR2 bei der Bildung von Lungenläsionen, der Pathogenabwehr sowie der Monozyten/Makophagen-Differenzierung nachgewiesen werden.

2.3 Ergebnisse

Im Folgenden werden die Ergebnisse der von mir veröffentlichten Studie zusammengefasst. Der Verweis auf im Folgenden erwähnte Abbildungen bezieht sich auf die in diesem veröffentlichten Artikel befindlichen und entsprechend nummerierten Abbildungen.

2.3.1 Verzögerte bakterielle Elimination, Symptomentwicklung und Makrophageninvasion in die Lunge bei CCR2-Defizienz

Die Erregerlasten in Lunge und Leber unterschieden sich an Tag 10 p.i. nicht zwischen CCR2-defizienten und Wildtyp-Mäusen, was auf eine ungehinderte Dissemination von der Haut in die inneren Organe hindeutet. Allerdings wiesen CCR2-defiziente Mäuse an Tag 14 und 17 p.i. in beiden Organen höhere Bakterienkonzentrationen auf, was auf eine beeinträchtigte Erreger-Clearance in Abwesenheit von CCR2-abhängigen-Monozyten schließen lässt (Figure 1B, Figure S1). Außerdem zeigten CCR2-defiziente Mäuse einen verzögerten Symptombeginn und Symptomerholung. Diese Verzögerung korrelierte auch mit einem verzögerten pulmonalen Einstrom von IBA1^{+}-Makrophagen

in die Lunge, welche eine Hauptkomponente der Lungeninfiltrate bei dieser Infektion darstellt und in denen *O. tsutsugamushi* nachgewiesen werden konnte (Figure 1D). Somit wurden in diesem Modell der *O. tsutsugamushi*-Infektion die bakterielle Clearance, die Symptomerholung sowie die Rekrutierung von Lungenmakrophagen durch eine CCR2-abhängige Zellpopulation vermittelt.

2.3.2 Gestörte Mobilisierung von Ly6C^{hi}- und Ly6C^{lo}-Monozyten bei CCR2-Defizienz

Bereits vor der Infektion mit *O. tsutsugamushi* wiesen Wildtyp-Tiere im Vergleich zu CCR2-defizienten Mäusen einen deutlich höheren relativen Anteil an CD11b^{+}-Ly6C^{hi}-Ly6G^{-}-Zellen im Blut auf, welcher zudem im Infektionsverlauf noch weiter anstieg (Figure 2B, C). Interessanterweise wiesen CCR2-defiziente Mäuse ebenfalls einen, wenn auch geringeren prozentualen Anstieg dieser Zellen im Blut auf. Allerdings wurde bei Wildtyp-Mäusen im weiteren Krankheitsverlauf eine 3-4-fach höhere und weiter steigende absolute Zellzahl von Ly6C^{hi}-Monozyten nachgewiesen, während diese bei den CCR2-defizienten Mäusen in absoluten Zahlen nicht und in relativen Zahlen deutlich geringer ausgeprägt war. Bemerkenswert ist, dass wider Erwarten auch die absolute Zahl von CD11b^{+}/Ly6C^{lo}-Monozyten CCR2-abhängig anstieg. Wildtyp-Mäuse zeigten während einer Infektion mit *O. tsutsugamushi* eine Rekrutierung sowohl von CD11b^{+} Ly6C^{hi}- als auch von CD11b^{+} Ly6C^{lo}-Monozyten im Blut. Bei CCR2-defizienten Mäusen hingegen wurde eine geringere und verzögerte Rekrutierung festgestellt, die nur in der relativen Menge der Ly6C^{hi}/Ly6C^{+}- Monozyten nachweisbar war. Die Monozytose im Blut ist somit weitgehend CCR2-abhängig, wobei Hinweise auf einen kleinen CCR2-unabhängigen Beitrag für die Rekrutierung von Ly6C^{hi}-Monozyten in das Blut gefunden wurden.

2.3.3 Pulmonale Infiltration von Ly6C^{hi}-Monozyten bei CCR2-defizienten Mäusen

Die Histopathologie deutete auf einen verzögerten Einstrom von Makrophagen in die Lunge bei CCR2-Defizienz hin (Figure 1D). Um diese Pneumonie phänotypisch und quantitativ zu charakterisieren, wurden auch hier CD11b-positive Ly6C^{hi}-, Ly6C^{lo}- und Ly6G^{+}- Zellen analysiert. Bei Wildtyp-Mäusen war der prozentuale Anteil von den CD11b^{+}- Ly6C^{hi} an allen Ly6C^{+}-Zellen vor Infektion bereits signifikant höher als bei CCR2-defizienten Mäusen, jedoch nicht während der *O. tsutsugamushi*-Infektion: Hier wiesen CCR2-defiziente Mäuse einen ähnlichen prozentualen Anteil an Ly6C^{hi}-Zellen in der Lunge auf (Figures 2B, C). Im Hinblick auf die absoluten Zahlen ließen sich aber Unterschiede zwischen den beiden Genotypen feststellen: Wildtyp-Mäuse zeigten im Vergleich zu CCR2-defizienten Mäusen eine 4-8-fach höhere Anzahl von Ly6C^{hi}-Monozyten in der Lunge (Figure 3C). Während des gesamten Verlaufs der *O. tsutsugamushi*-Infektion waren diese Unterschiede signifikant. Außerdem exprimierten über 90% der CD11b^{+}/Ly6C^{hi}-Zellen beider Genotypen den Makrophagenmarker F4/80. Die Expression von MHCII durch diese-Zellen lag bei nicht infizierten Mäusen zwischen 10-20 % und stieg während der Infektion auf über 80 % an. Zusätzlich wurde eine schnellere Hochregulierung von MHCII in Wildtyp-Mäusen beobachtet

(Figure S2A, B). Diese Daten legen nahe, dass die Rekrutierung von CD11b^{+}/Ly6C^{hi}-Monozyten/Makrophagen in die Lunge CCR2 erfordert.

2.3.4 Pulmonale Infiltration von Ly6C^{lo}-Monozyten bei CCR2-defizienten Mäusen

Auffällig zeigte sich auch eine Ly6C^{lo}-Population in der Lunge. Zwischen 80-90 % der Ly6C^{lo}-Zellen vor der Infektion exprimierten den Makrophagenmarker F4/80. Die relativen Anteile der F4/80-exprimierenden Ly6C^{lo}-Zellen unterschieden sich auch während der Infektion nicht signifikant zwischen Wildtyp- und CCR2-defizienten Mäusen. Während die absolute Anzahl der pulmonalen Ly6C^{lo}-F4/80^{+}-Makrophagen bei beiden Genotypen am Tag 0 vergleichbar war, stieg sie bei Wildtyp-Mäusen unter der Infektion im Vergleich zu CCR2-defizienten Mäusen signifikant an (Figure 4A). Die MHCII-Expression auf Ly6C^{lo}-Zellen stieg von 20-40 % auf etwa 80-90 % an, was auf einen aktivierten Makrophagen-Phänotyp schließen lässt. Die absolute Zahl entsprechender Zellen war auch hier in Wildtypen-Mäusen signifikant höher (Figure 4C). Eine Koexpressionsanalyse zeigte, dass MHCII während der Infektion hauptsächlich von F4/80^{+}-Zellen exprimiert wurde. Auch die doppelt positive F4/80/MHCII-Makrophagenpopulation nahm bei Wildtyp-Mäusen früher zu. Bei CCR2-defizienten Mäusen gab es zwar keinen Defekt bei der Hochregulierung der Expression von F4/80/MHCII auf Ly6C^{lo}-Zellen, die Population war bei Wildtyp-Mäusen im Vergleich aber 5-10-mal größer (Figure 4C).

Es möglich ist, dass sich die Ly6C^{lo}-Monozyten nach Migration in das Zielgewebe durch Differenzierung aus den stark CCR2-exprimierenden Ly6C^{hi}-Monozyten entwickelt haben. Denkbar ist auch, dass ihre Rekrutierung direkt über CCR2-abhängige Mechanismen erfolgte. Um frühere Beobachtungen zu bestätigen, dass auch Ly6C^{lo}-Zellen CCR2 exprimieren, wurde die Expression von CCR2 auf Ly6C^{hi}- und Ly6C^{lo}-Blutmonozyten gemessen. Ly6C^{lo}-Monozyten von Wildtyp-Mäusen hatten eine höhere mittlere Fluoreszenz-Intensität (MFI) in der CCR2-Färbung als die von CCR2-defizienten Mäusen oder ungefärbten Kontrollen, was eine geringe CCR2-Expression zeigt (Figures S3C, D). Die effiziente Rekrutierung sowohl von Ly6C^{hi}- als auch von Ly6C^{lo}-Monozyten/Makrophagen in die Lunge von *O. tsutsugamushi*-infizierten Mäusen erforderte also CCR2. Der Defekt bei der CCR2-abhängigen Rekrutierung von Monozyten/Makrophagen verlief dabei parallel zur beeinträchtigten bakteriellen Clearance in CCR2-defizienten Mäusen.

2.3.5 Monozyten-Populationen und Clearance in der Milz

Die Induktion einer kleinen Population von Ly6C^{hi}-Monozyten im Blut und Ly6C^{hi}- sowie Ly6C^{lo}-Monozyten/Makrophagen in die Lunge unter CCR2-Defiezienz war überraschend und deutete auf eine CCR2-unabhängige Quelle dieser Zellen hin. Es konnte bereits gezeigt werden, dass die Milz als alternatives Reservoir für Ly6C^{hi}-Monozyten dienen kann, die sekundär weitere Organe wie etwa das Herz infiltrieren können (Swirski, Nahrendorf et al. 2009, Hettinger, Richards et al. 2013). Es wurde daher die Ly6C^{hi}-Monozytenpopulation in der Milz von infizierten Mäusen untersucht. Ein Unterschied im prozentualen Anteil von Ly6C^{hi}/Ly6C^{+}-Zellen und in der Größe der Ly6C^{hi}-

Monozytenpopulation wurde nur vor der Infektion festgestellt: Während der Infektion zeigten sich weder prozentual noch absolut signifikante Unterschiede (Figures S4A, B). Interessanterweise sank der Prozentsatz der Ly6C^{hi}-Zellen in der Milz nach dem 14. Infektionstag rascher als in der Lunge. Dies ging in CCR2-defizienten- und Wildtyp-Mäusen mit einer vergleichbaren bakteriellen Clearance aus der Milz einher (Figure S4C). Das unauffällige Verhalten der Ly6C^{hi}-Monozyten-Population in der Milz von CCR2-defizienten Mäusen zeigte also, dass die Rekrutierung von Ly6C^{hi}-Monozyten in der Milz im Gegensatz zur Lunge CCR2-unabhängig war. Diese splenische Ly6C^{hi}-Population könnte möglicherweise eine alternative Quelle für Monozyten in Blut und Lunge darstellen.

2.3.6 Inflammatorisches Zytokinmilieu in der Lunge

Um das Zytokinmilieu im Lungengewebe zu charakterisieren, wurde die Transkription von M1-assoziierten (iNOS, TNF-α, IFN-γ) und M2-assoziierten Genen (IL-4 und ARG1) sowie von CCL2 mittels quantitativer real time-PCR gemessen. Alle Gene waren in beiden Genotypen während der Infektion mit *O. tsutsugamushi* hochreguliert (Figure 5). Die Induktion der M1-assoziierten Gentranskription war jedoch bei CCR2-defizienten Mäusen unter der Infektion signifikant verzögert. Auch die M2-assoziierte Gentranskription war in CCR2-dezienten Mäusen verzögert. Dies deutet darauf hin, dass die Entwicklung eines entzündlichen Zytokinmilieus in Abwesenheit von CCR2 später erfolgt. Diese Verzögerung war wiederum mit einem späteren Einstrom von Makrophagen in die Lunge assoziiert.

2.3.7 Infiltration von Makrophagen im Lungenparenchym und im Bronchus-assoziierten lymphatischen Gewebe (BALT)

Es stellte sich die Frage, ob eine CCR2-Defizienz die histologische Lokalisation von Makrophagen in der Lunge während einer *O. tsutsugamushi*-Infektion beeinflusst. Zu diesem Zweck wurde eine immunhistochemische Untersuchung des Makrophagenmarkers IBA1 an Formalin-Fixed-Paraffin-Embedded (FFPE)-Schnitten von Lungengewebe durchgeführt. Das Parenchym von Wildtyp-Mäusen wurde im Vergleich zu CCR2-defizienten Mäusen von IBA1-positiven Makrophagen stärker infiltriert. Die IBA1-positive Fläche wurde quantifiziert und zeigte sich im Lungenparenchym bei Wildtyp-Mäusen signifikant größer. In der späten Infektionsphase wurde jedoch auch eine Infiltration des Lungenparenchyms in CCR2-defizienten Mäuse deutlich, was darauf hindeutet, dass CCR2-unabhängige Signale den zunächst beobachteten Defekt kompensieren und eine spätere Infiltration von Makrophagen in das Lungenparenchym ermöglichen. Es konnte auch beobachtet werden, dass sich dieser Effekt auf das Parenchym beschränkte, da die peribronchialen (BALT-) Bereiche in beiden Genotypen ähnlich infiltriert waren (Figure 6).

2.3.8 Diskussion

Während zunächst die Vermutung nahe lag, dass entzündliche Monozyten, die sich später zu Makrophagen differenzieren können, die Verbreitung von *O. tsutsugamushi* in vom Inokulationsort

entfernte Organe vermitteln könnten, musste diese Hypothese angesichts der gleichen oder sogar erhöhten Bakterienkonzentrationen in CCR2-defizienten Mäusen in Lunge, Leber und Milz verworfen werden. Angesichts der verringerten Monozytose im Blut und des Beginns des Makrophageneinstroms in das Lungengewebe um Tag 10 p.i. ist es unwahrscheinlich, dass CCR2-abhängige Mechanismen bei der Bakterienbeseitigung vor diesem Zeitpunkt eine Rolle spielen. Im Gegensatz zu bisherigen Studien mit anderen Erregern zeigt diese Arbeit, dass CCR2 in diesem Modell für eine suffiziente Infektabwehr nicht zwingend erforderlich ist, diese jedoch beschleunigt. Als Einschränkung dieser Studie kann nicht ausgeschlossen werden, dass andere Inokulationswege, höhere Infektionsdosen oder Infektionen bei männlichen Mäusen (männliche Mäuse exprimieren in nicht-klassischen Milzmonozyten höhere Mengen an CCR2 (Kay, Gomez-Garcia et al. 2015)) einen anderen Infektionsverlauf hervorrufen könnten. CCR2-defiziente Mäuse zeigten eine signifikant reduzierte Rekrutierung von Ly6C^{hi}- und Ly6C^{lo}-Monozyten in die Lunge, eine verzögerte Infiltration von IBA1^{+}-Zellen in das Lungenparenchym, eine verzögerte Entwicklung des entzündlichen Zytokinmilieus und eine verzögerte klinische Erholung. Die Rekrutierung der Monozyten aus dem Blut in die Lunge ist vermutlich ein mittelbarer Effekt der CCR2-abhängigen Monozytose, der hier nicht unabhängig untersucht wurde. Um die Rolle von CCR2 bei der Auswanderung von Ly6C^{hi}-Monozyten aus dem Blut in die Lunge zu untersuchen, wären adoptive-Transfer-Experimente, nach Sortierung von CD115-positiven Monozyten aus dem Knochenmark oder der Milz, erforderlich. Arbeiten mit *Listeria monocytogenes* konnten jedoch zeigen, dass die Rekrutierung aus dem Blut zum Infektionsort unabhängig von CCR2 stattfindet (Shi, Velázquez et al. 2010). Bemerkenswerterweise gab es keinen Defekt der bakteriellen Clearance in der Milz, wo eine ungestörte Expansion von Ly6C^{hi}- und Ly6C^{lo}-Monozyten in CCR2-defizienten Mäusen gefunden wurde. Die Ergebnisse deuten darauf hin, dass bei einer *O. tsutsugamushi*-Infektion in Abwesenheit von CCR2 eine kleine, aber möglicherweise ausreichende Anzahl von Monozyten rekrutiert werden kann, entweder aus anderen Organen als dem Knochenmark, vielleicht der Milz, oder über andere Rezeptoren. Somit könnten auch CCR2-unabhängigen Mechanismen ausreichen, um diese Infektion zu bewältigen. Es konnte hier experimentell nachgewiesen werden, dass die interstitielle IBA1^{+}-Makrophagenentzündung in der Lunge CCR2-abhängig war, während die peribronchial infiltrierenden Makrophagen CCR2-unabhängig waren. Diese Zellen könnten eine alternative lokale Quelle für Makrophagen sein, die später in das Lungenparenchym einwandern. Tatsächlich stammen nicht alle Gewebsmonozyten oder Makrophagen, die sich während einer Infektion vermehren, von Blutmonozyten ab, die über CCR2 aus dem Knochenmark rekrutiert werden: Jenkins et al. haben gezeigt, dass sich Makrophagen als Reaktion auf IL-4 lokal und knochenmarkunabhängig in der Pleurahöhle vermehren können (Jenkins, Ruckerl et al. 2011). Auch hier wurde ein signifikanter Anstieg der lokalen IL-4-mRNA-Transkription in der Lunge in CCR2-defizienten Mäusen gemessen, wenn auch später als in Wildtyp-Mäusen. Es wird daher von Interesse sein, in Zukunft die Mechanismen der knochenmarkunabhängigen Makrophagenentzündung bei der

O. tsutsugamushi-Infektion zu untersuchen, z. B. die Rolle der IL-4-getriebenen lokalen Proliferation oder der Rekrutierung aus der Milz. Interessant ist, dass die Induktion von Th2-Zytokinen offenbar vom Infektionsweg abhängt: Bei einem intravenösen Infektionsmodell von *O. tsutsugamushi*, das eine rasche Ausbreitung des Erregers ermöglicht, wurde die Transkription von IL-4- und IL-13-mRNA unterdrückt und somit als gestörte Th2-Reaktion interpretiert (Soong, Wang et al. 2014). In den Lungen von intradermal infizierten Mäusen wiesen Soong et al. jedoch neben TH1-verwandten Zytokinen auch IL-13 nach, was auf eine gemischte Th1/Th2-Antwort schließen lässt (Soong, Mendell et al. 2016). Die präsentierten Daten zeigen, dass die CCR2-Defizienz die Polarisierung bei einer *O. tsutsugamushi*-Infektion nicht vollständig in Richtung eines Pols verschiebt, sondern vielmehr den oben erwähnten gemischten Phänotyp verzögert. Dies unterscheidet sich von der Infektion mit *Cryptococcus neoformans*, bei der die CCR2-Defizienz die Polarisierung vollständig von Th1 zu Th2 verschoben hat (Traynor, Kuziel et al. 2000). Entgegen der Erwartung ließ sich feststellen, dass der CCR2-knock-out nicht nur die Ly6C^{hi}-Monozyten, sondern auch die Ly6C^{lo}-Monozyten betraf. Auch die Expression von MHCII und F4/80 auf pulmonalen Ly6C^{lo}-Monozyten war während der Infektion in CCR2-defizienten Mäusen signifikant verringert. Es zeigt sich, dass CCR2 während einer *O. tsutsugamushi*-Infektion nicht nur erforderlich ist, um eine systemische Ly6C^{hi}-Monozytenreaktion auszulösen, sondern auch, um eine Ly6C^{lo}-Monozytose und die Induktion einer pulmonalen Ly6C^{lo}-Monozytenpopulation zu induzieren. Es gibt mindestens zwei Faktoren, die hierzu beitragen könnten: Die Expression von Ly6C^{lo}-Monozyten könnte direkt durch CCR2 reguliert werden. Ly6C^{lo}-Monozyten könnten aber auch von CCR2-abhängigen Ly6C^{hi}-Monozyten abstammen. Für den ersten Mechanismus sprechen Studien, die zeigen, dass Ly6C^{lo}-Monozyten eine geringe Expression von CCR2 aufweisen (Schmid, Harris 2014), was auch in dieser Arbeit bestätigt wurde. Diese geringe Expression von CCR2 könnte zu ihrem Austritt aus dem Knochenmark beitragen. Wichtiger ist jedoch, dass Ly6C^{hi}-Monozyten obligatorische Vorläufer von Ly6C^{lo}-Zellen in Blut und Gewebe darstellen (Varga, Mounier et al. 2013, Yona, Kim et al. 2013, Hilgendorf, Gerhardt et al. 2014, Dal-Secco, Wang et al. 2015). Es wurde gezeigt, dass der Übergang von CCR2^{hi}/CX$_3$CR1^{lo}- zu CX$_3$CR1^{hi}/CCR2^{lo}-Monozyten durch die lokale Produktion der Zytokine IL-4 und IL-10 vermittelt wird. Yona et al. wiesen in einer gemischten Knochenmarkschimäre nach, dass die Bildung peripherer Ly6C^{lo}-Monozyten im steady-state entscheidend von CCR2-kompetenten Ly6C^{hi}-Zellen als deren unmittelbaren Vorläufern abhängt, die aus dem Knochenmark mobilisiert werden müssen. Die Beobachtung, dass CCR2-defiziente Mäuse dennoch zirkulierende Ly6C^{lo}-Monozyten beherbergen, konnte durch eine verlängerte Lebensdauer von Ly6C^{lo}-Monozyten in Abwesenheit von Ly6C^{hi}-Monozyten erklärt werden. Es ist daher wahrscheinlich, dass sich bei einer *O. tsutsugamushi*-Infektion eine große Anzahl an Ly6C^{lo}-Monozyten von ihrem CCR2-abhängigen Ly6C^{hi}-Vorläufer differenziert, was zu einer beeinträchtigten Reaktion beider Untergruppen in CCR2-defizienten Mäusen führt. Die verzögerte Kinetik der Ly6C^{lo}-Antwort im Vergleich zur Ly6C^{hi}-Antwort bei einer *O. tsutsugamushi*-Infektion unterstützt diese Annahme.

Bemerkenswert ist, dass die Monozytenreaktion und die Bakterienbeseitigung in unserem Modell in der Milz unabhängig von CCR2 waren. Diese Monozyten können aus gemeinsamen Monozytenvorläufern (cMoP) in der Milz hervorgehen, einem hochgradig proliferativen Zelltyp, aus dem verschiedene Monozytenuntergruppen und Makrophagen entstehen können (Hettinger, Richards et al. 2013). Für die Beseitigung von *O. tsutsugamushi* aus der Milz scheinen diese lokalen Milzmechanismen ausreichend zu sein, ohne dass Monozyten aus dem Knochenmark über CCR2 rekrutiert werden müssen.

2.4 Literaturverzeichnis

Astrup, E., et al. (2014). "Cytokine network in scrub typhus: high levels of interleukin-8 are associated with disease severity and mortality." PLoS Negl Trop Dis **8**(2): e2648.

Auffray, C., et al. (2007). "Monitoring of blood vessels and tissues by a population of monocytes with patrolling behavior." Science **317**(5838): 666-670.

Biswas, A., et al. (2015). "Ly6C(high) monocytes control cerebral toxoplasmosis." J Immunol **194**(7): 3223-3235.

Boring, L., et al. (1998). "Decreased lesion formation in CCR2-/- mice reveals a role for chemokines in the initiation of atherosclerosis." Nature **394**(6696): 894-897.

Chen, H. C., et al. (2012). "Chest radiographic presentation in patients with scrub typhus." Trans R Soc Trop Med Hyg **106**(1): 48-53.

Chi, W. C., et al. (1997). "Scrub typhus associated with multiorgan failure: a case report." Scand J Infect Dis **29**(6): 634-635.

Cho, N. H., et al. (2001). "Expression of chemokine genes in human dermal microvascular endothelial cell lines infected with *Orientia tsutsugamushi*." Infect Immun **69**(3): 1265-1272.

Cho, N. H., et al. (2000). "Expression of chemokine genes in murine macrophages infected with *Orientia tsutsugamushi*." Infect Immun **68**(2): 594-602.

Cho, N. H., et al. (2002). "Induction of the gene encoding macrophage chemoattractant protein 1 by *Orientia tsutsugamushi* in human endothelial cells involves activation of transcription factor activator protein 1." Infect Immun **70**(9): 4841-4850.

Crane, M. J., et al. (2014). "The monocyte to macrophage transition in the murine sterile wound." PLoS ONE **9**(1): e86660.

Dal-Secco, D., et al. (2015). "A dynamic spectrum of monocytes arising from the in situ reprogramming of CCR2+ monocytes at a site of sterile injury." J Exp Med **212**(4): 447-456.

Epelman, S., et al. (2014). "Embryonic and adult-derived resident cardiac macrophages are maintained through distinct mechanisms at steady state and during inflammation." Immunity **40**(1): 91-104.

Epelman, S., et al. (2014). "Origin and functions of tissue macrophages." Immunity **41**(1): 21-35.

Gautier, E. L., et al. (2012). "Gene-expression profiles and transcriptional regulatory pathways that underlie the identity and diversity of mouse tissue macrophages." Nat Immunol **13**(11): 1118-1128.

Ginhoux, F. and S. Jung (2014). "Monocytes and macrophages: developmental pathways and tissue homeostasis." Nat Rev Immunol **14**(6): 392-404.

Gomez Perdiguero, E., et al. (2015). "Tissue-resident macrophages originate from yolk-sac-derived erythro-myeloid progenitors." Nature **518**(7540): 547-551.

Gordon, S., et al. (2011). "F4/80 and the related adhesion-GPCRs." Eur J Immunol **41**(9): 2472-2476.

Gordon, S. and F. O. Martinez (2010). "Alternative activation of macrophages: mechanism and functions." Immunity **32**(5): 593-604.

Groves, M. G. and D. J. Kelly (1989). "Characterization of factors determining *Rickettsia tsutsugamushi* pathogenicity for mice." Infect Immun **57**(5): 1476-1482.

Guilliams, M., et al. (2013). "Alveolar macrophages develop from fetal monocytes that differentiate into long-lived cells in the first week of life via GM-CSF." J Exp Med **210**(10): 1977-1992.

Hashimoto, D., et al. (2013). "Tissue-resident macrophages self-maintain locally throughout adult life with minimal contribution from circulating monocytes." Immunity **38**(4): 792-804.

Hauptmann, M., et al. (2016). "Protective and Pathogenic Roles of CD8+ T Lymphocytes in Murine *Orientia tsutsugamushi* Infection." PLoS Negl Trop Dis **10**(9): e0004991.

Helk, E., et al. (2013). "TNFα-mediated liver destruction by Kupffer cells and Ly6Chi monocytes during *Entamoeba histolytica* infection." PLoS Pathog **9**(1): e1003096.

Hettinger, J., et al. (2013). "Origin of monocytes and macrophages in a committed progenitor." Nat Immunol **14**(8): 821-830.

Hilgendorf, I., et al. (2014). "Ly-6Chigh monocytes depend on Nr4a1 to balance both inflammatory and reparative phases in the infarcted myocardium." Circ Res **114**(10): 1611-1622.

Italiani, P. and D. Boraschi (2014). "From Monocytes to M1/M2 Macrophages: Phenotypical vs. Functional Differentiation." Front Immunol **5**: 514.

Jenkins, S. J., et al. (2011). "Local macrophage proliferation, rather than recruitment from the blood, is a signature of TH2 inflammation." Science **332**(6035): 1284-1288.

Jeong, Y. J., et al. (2007). "Scrub typhus: clinical, pathologic, and imaging findings." Radiographics **27**(1): 161-172.

Jiang, J. and A. L. Richards (2018). "Scrub Typhus: No Longer Restricted to the Tsutsugamushi Triangle." Trop Med Infect Dis **3**(1).

Kay, E., et al. (2015). "Sexual dimorphisms in leukocyte trafficking in a mouse peritonitis model." J Leukoc Biol **98**(5): 805-817.

Keller, C. A., et al. (2014). "Dissemination of *Orientia tsutsugamushi* and inflammatory responses in a murine model of scrub typhus." PLoS Negl Trop Dis **8**(8): e3064.

Kelly, D. J., et al. (2009). "Scrub typhus: the geographic distribution of phenotypic and genotypic variants of *Orientia tsutsugamushi*." Clin Infect Dis **48 Suppl 3**: S203-230.

Kim, H. (2017). "The transcription factor MafB promotes anti-inflammatory M2 polarization and cholesterol efflux in macrophages." Sci Rep **7**(1): 7591.

Kurihara, T., et al. (1997). "Defects in macrophage recruitment and host defense in mice lacking the CCR2 chemokine receptor." J Exp Med **186**(10): 1757-1762.

Liu, M., et al. (2020). "Transcription factor c-Maf is a checkpoint that programs macrophages in lung cancer." J Clin Invest **130**(4): 2081-2096.

Luce-Fedrow, A., et al. (2018). "A Review of Scrub Typhus (*Orientia tsutsugamushi* and Related Organisms): Then, Now, and Tomorrow." Trop Med Infect Dis **3**(1).

MacMicking, J., et al. (1997). "Nitric oxide and macrophage function." Annu Rev Immunol **15**: 323-350.

Martinez, F. O. and S. Gordon (2014). "The M1 and M2 paradigm of macrophage activation: time for reassessment." F1000Prime Rep **6**: 13.

Martinez, F. O., et al. (2008). "Macrophage activation and polarization." Front Biosci **13**: 453-461.

Mills, C. D. (2012). "M1 and M2 Macrophages: Oracles of Health and Disease." Crit Rev Immunol **32**(6): 463-488.

Murray, P. J. and T. A. Wynn (2011). "Protective and pathogenic functions of macrophage subsets." Nat Rev Immunol **11**(11): 723-737.

Nahrendorf, M., et al. (2007). "The healing myocardium sequentially mobilizes two monocyte subsets with divergent and complementary functions." J Exp Med **204**(12): 3037-3047.

Paris, D. H., et al. (2012). "*Orientia tsutsugamushi* in human scrub typhus eschars shows tropism for dendritic cells and monocytes rather than endothelium." PLoS Negl Trop Dis **6**(1): e1466.

Peters, W., et al. (2001). "Chemokine receptor 2 serves an early and essential role in resistance to *Mycobacterium tuberculosis*." Proc Natl Acad Sci U S A **98**(14): 7958-7963.

Rath, M., et al. (2014). "Metabolism via Arginase or Nitric Oxide Synthase: Two Competing Arginine Pathways in Macrophages." Front Immunol **5**: 532.

Rivollier, A., et al. (2012). "Inflammation switches the differentiation program of Ly6Chi monocytes from antiinflammatory macrophages to inflammatory dendritic cells in the colon." J Exp Med **209**(1): 139-155.

Sasaki, Y., et al. (2001). "Iba1 is an actin-cross-linking protein in macrophages/microglia." Biochem Biophys Res Commun **286**(2): 292-297.

Schmid, M. A. and E. Harris (2014). "Monocyte recruitment to the dermis and differentiation to dendritic cells increases the targets for *dengue virus* replication." PLoS Pathog **10**(12): e1004541.

Scott, C. L., et al. (2016). "Bone marrow-derived monocytes give rise to self-renewing and fully differentiated Kupffer cells." Nat Commun **7**: 10321.

Serbina, N. V., et al. (2008). "Monocyte-mediated defense against microbial pathogens." Annu Rev Immunol **26**: 421-452.

Serbina, N. V. and E. G. Pamer (2006). "Monocyte emigration from bone marrow during bacterial infection requires signals mediated by chemokine receptor CCR2." Nat Immunol **7**(3): 311-317.

Serbina, N. V., et al. (2003). "TNF/iNOS-producing dendritic cells mediate innate immune defense against bacterial infection." Immunity **19**(1): 59-70.

Serbina, N. V., et al. (2012). "Monocyte-mediated immune defense against murine *Listeria monocytogenes* infection." Adv Immunol **113**: 119-134.

Shi, C., et al. (2011). "Bone marrow mesenchymal stem and progenitor cells induce monocyte emigration in response to circulating toll-like receptor ligands." Immunity **34**(4): 590-601.

Shi, C. and E. G. Pamer (2011). "Monocyte recruitment during infection and inflammation." Nat Rev Immunol **11**(11): 762-774.

Shi, C., et al. (2010). "Monocyte trafficking to hepatic sites of bacterial infection is chemokine independent and directed by focal intercellular adhesion molecule-1 expression." J Immunol **184**(11): 6266-6274.

Sica, A. and A. Mantovani (2012). "Macrophage plasticity and polarization: in vivo veritas." J Clin Invest **122**(3): 787-795.

Song, S. W., et al. (2004). "Clinical role of interstitial pneumonia in patients with scrub typhus: a possible marker of disease severity." J Korean Med Sci **19**(5): 668-673.

Soong, L., et al. (2016). "An Intradermal Inoculation Mouse Model for Immunological Investigations of Acute Scrub Typhus and Persistent Infection." PLoS Negl Trop Dis **10**(8): e0004884.

Soong, L., et al. (2014). "Strong type 1, but impaired type 2, immune responses contribute to *Orientia tsutsugamushi*-induced pathology in mice." PLoS Negl Trop Dis **8**(9): e3191.

Swirski, F. K., et al. (2009). "Identification of splenic reservoir monocytes and their deployment to inflammatory sites." Science **325**(5940): 612-616.

Tamoutounour, S., et al. (2013). "Origins and functional specialization of macrophages and of conventional and monocyte-derived dendritic cells in mouse skin." Immunity **39**(5): 925-938.

Traynor, T. R., et al. (2000). "CCR2 expression determines T1 versus T2 polarization during pulmonary *Cryptococcus neoformans* infection." J Immunol **164**(4): 2021-2027.

Trent, B., et al. (2020). "Polarized lung inflammation and Tie2/angiopoietin-mediated endothelial dysfunction during severe *Orientia tsutsugamushi* infection." PLoS Negl Trop Dis **14**(3): e0007675.

Varga, T., et al. (2013). "Tissue LyC6- macrophages are generated in the absence of circulating LyC6- monocytes and Nur77 in a model of muscle regeneration." J Immunol **191**(11): 5695-5701.

Vogel, D. Y., et al. (2013). "Macrophages in inflammatory multiple sclerosis lesions have an intermediate activation status." J Neuroinflammation **10**: 35.

Wangrangsimakul, T., et al. (2020). "Scrub Typhus and the Misconception of Doxycycline Resistance." Clin Infect Dis **70**(11): 2444-2449.

Yona, S., et al. (2013). "Fate mapping reveals origins and dynamics of monocytes and tissue macrophages under homeostasis." Immunity **38**(1): 79-91.

Yunna, C., et al. (2020). "Macrophage M1/M2 polarization." Eur J Pharmacol **877**: 173090.

3. Zusammenfassung

In der vorliegenden Studie wurde zum ersten Mal der Mechanismus der CCR2-abhängigen Rekrutierung von Monozyten in das Blut und das Lungengewebe in einem Mausmodell (C57BL/6) der selbstheilenden *O. tsutsugamushi*-Infektion untersucht. Es konnte gezeigt werden, dass die Clearance von *O. tsutsugamushi* in Abwesenheit von CCR2 in der Lunge (und auch in der Leber) deutlich weniger effektiv und verzögert war. CCR2-defiziente Mäuse waren aber in der Lage, die Infektion zu kontrollieren. Die Beseitigung der Bakterien aus der Lunge, die Entwicklung interstitieller pulmonaler Gewebeläsionen und die Entwicklung eines Entzündungsmilieus waren in Abwesenheit von CCR2 jedoch deutlich verzögert. CCR2 war für die Mobilisierung von Monozyten im Blut erforderlich und verstärkte den Zustrom von $Ly6C^{hi}$-Monozyten in die Lunge, von denen die meisten einen aktivierten Makrophagen-Phänotyp entwickelten. Unerwarteterweise gab es auch eine klare Abhängigkeit der pulmonalen $Ly6C^{lo}$-Monozyten/Makrophagen-Population von CCR2, während die Neutrophilen davon unberührt blieben. Es konnte auch gezeigt werden, dass die frühe interstitielle Infiltration des Lungenparenchyms durch $IBA1^{+}$-Makrophagen CCR2-abhängig war, während die Entwicklung der Peribronchitis CCR2-unabhängig war. Im Gegensatz dazu wurden die Ausbreitung der $Ly6C^{hi}$- und $Ly6C^{lo}$- Populationen und die bakterielle Clearance in der Milz durch den CCR2-Mangel nicht beeinflusst. Die vorliegenden Daten deuten darauf hin, dass CCR2 die zeitlich-räumliche Rekrutierung und Aktivierung von Monozyten und Makrophagen in der Lunge steuert und damit lokal zur Kontrolle der *O. tsutsugamushi*-Infektion beiträgt. In Übereinstimmung mit diesen Ergebnissen verzögerte der CCR2-Mangel auch die Entwicklung klinischer Symptome, was auf eine immunpathologische Rolle der entzündlichen Monozyten hindeutet.

Summary

In the present study, the mechanism of CCR2-dependent recruitment of monocytes to the blood and lung tissue was investigated for the first time in a mouse model (C57BL/6) of self-healing *O. tsutsugamushi* infection. It was shown that clearance of *O. tsutsugamushi* was significantly less effective and delayed in the absence of CCR2 in the lung (and also in the liver). CCR2-deficient mice were able to control infection, but clearance of bacteria from the lung, development of interstitial pulmonary tissue lesions, and development of an inflammatory milieu were significantly delayed in the absence of CCR2. CCR2 was required for the mobilization of monocytes in the blood and enhanced the influx of $Ly6C^{hi}$ monocytes into the lungs, most of which developed an activated macrophage phenotype. Unexpectedly, there was also a clear dependence of the pulmonary $Ly6C^{lo}$ monocyte/macrophage population on CCR2, whereas the number of neutrophils was unaffected. It was also shown that early interstitial infiltration of the lung parenchyma by $IBA1^{+}$ macrophages was CCR2-dependent, whereas the development of peribronchitis was CCR2-independent. In contrast, the spread of $Ly6C^{hi}$ and $Ly6C^{lo}$ populations and bacterial clearance in the spleen were not affected by CCR2 deficiency. This data suggest that CCR2 controls the temporospatial recruitment and activation of monocytes and macrophages in the lung and thus contributes locally to the control of

O. tsutsugamushi infection. Consistent with these findings, CCR2 deficiency also delayed the development of clinical symptoms, suggesting an immunopathologic role for inflammatory monocytes.

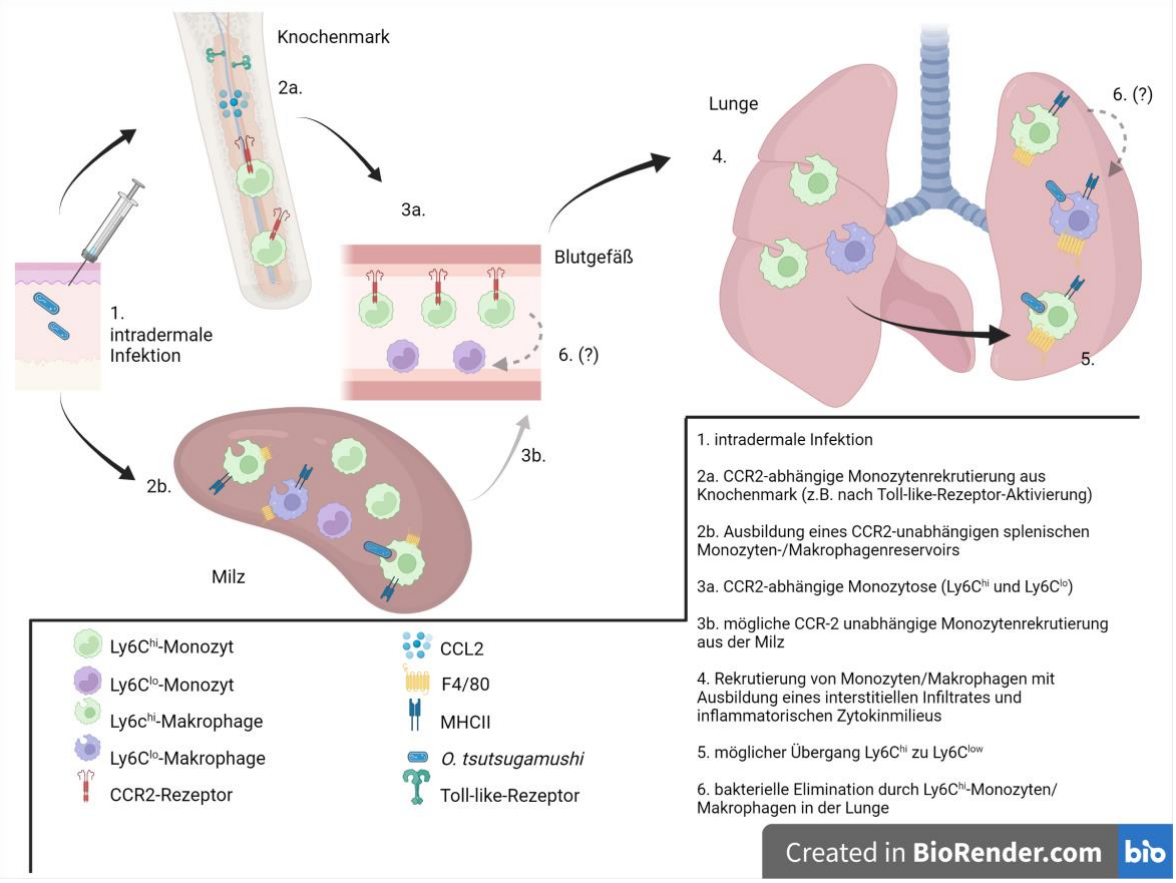

Abbildung 1: *zusammenfassende Illustration der Arbeitshypothese: CCR2-abhängige Monozyten- und Makrophagen-Reaktion nach einer intradermalen O. tsutsugamushi-Infektion*

4. Erklärung des Eigenanteils

Bis auf wenige im folgenden genannte Ausnahmen wurden die experimentellen, graphischen und statistischen Auswertungen von mir durchgeführt. Die Infektion, klinische Begutachtung, Organ- und Blutentnahme sowie die Tötung der Tiere habe ich geplant und im Anschluss gemeinsam mit PD Dr. C. Keller (Institut für Virologie, Universitätsklinikum Marburg) vollzogen, die Organ- und Zellaufbereitung für sämtliche weitere Analyseschritte, insbesondere auch Durchflusszytometrie-Messungen, mRNA-Aufbereitung und -Nachweis sowie Erregernachweis mittels PCR sowie hierfür alle vorbereitende Laborarbeiten habe ich selbstständig durchgeführt. Ich habe die histologischen Proben mit Ausnahme der Immunfluoreszenzfärbung (PD Dr. C. Keller, Institut für Virologie, Universitätsklinikum Marburg) nach histologischer Aufarbeitung (durch das Institut für Neuropathologie am Universitätsklinikum Eppendorf unter Leitung von Prof. Dr. M. Glatzel) aufbereitet und fotografiert, die Quantifizierung und statistische Auswertung dieser Proben erfolgte durch Dr. Z. Orfanos (Institut für Virologie, Universitätsklinikum Marburg). Die Aufbereitung der Proben und Zellen für die Durchflusszytometrie, Durchführung und Auswertung der Durchflusszytometrie mit Ausnahme der CCR2-Expressionsanalyse (Dr. Julie Sellau, Abteilung für Molekularbiologie und Immunologie, Bernhard-Nocht-Institut für Tropenmedizin Hamburg) aus den entsprechenden Organen sowie Isolation von DNA und mRNA, Durchführung der reversen Transkription und qualitativen RT-PCR inklusive Auswertung zur Gen-Expressionsanalysen und Erregerlastbestimmung erfolgten durch mich. Die statistische Auswertung, graphische Darstellung und Verschriftlichung der vorliegenden Arbeit habe ich unter Anleitung von und in Zusammenarbeit mit PD Dr. Christian Keller durchgeführt.

5. Danksagung

Ich danke in erster Linie dem Bernhard-Nocht-Institut für Tropenmedizin Hamburg und allen an dieser Arbeit beteiligten Personen, im Speziellen Dr. Zacharias Orfanos, Dr. Julie Sellau, Mohammad Gharaibeh, Ute Mehlhoop und Hannelore Lotter. Besonderer Dank geht an meinen Doktorvater Prof. Dr. Bernhard Fleischer und meinen Doktorandenbetreuer PD Dr. Christian Keller, außerdem an die „Vereinigung der Freunde des Tropeninstituts Hamburg e. v." für die Unterstützung mit einem Stipendium während der Arbeit. Darüber hinaus danke ich Jakob Schwemmler für viele lange Tage im Labor.

6. Lebenslauf

Lebenslauf aus datenschutzrechtlichen Gründen nicht enthalten

7. Abkürzungsverzeichnis

- ARG1 Arginase 1
- BALT bronchus-associated lymphoid tissues
- CCL CC-Chemokinligand
- CCR2 C-C chemokine receptor type 2
- CX_3CR1^{hi} CX3C chemokine receptor 1 high expression
- CX_3CR1^{lo} CX3C chemokine receptor 1 low expression
- CD11b Cluster of Differentiation 11b
- CD115 Cluster of Differentiation 115
- cMoP common monocyte precursors
- IBA1 Ionized calcium-binding adapter molecule 1
- IFN Interferon
- IL Interleukin
- iNOS Inducible Nitric Oxide Synthase
- $Ly6C^{hi}$ lymphocyte antigen 6 complex high expression
- $Ly6C^{lo}$ lymphocyte antigen 6 complex low expression
- Ly6G Lymphocyte antigen 6 complex locus G6D
- MFI mean flourescence intensity
- MHC major histocompatibility complex
- mRNA messenger ribonucleic acid
- O. tsutsugamushi Orientia tsutsugamushi
- PCR polymerase chain reaction
- p.i. post infection
- Tip-DC TNF/iNos-producing Dendritic Cells
- Th1/2 T helper type 1/2
- TLR Toll-like-Rezeptor
- TNF Tumornekrosefaktor

8. Eidesstattliche Versicherung

Ich versichere ausdrücklich, dass ich die Arbeit selbständig und ohne fremde Hilfe verfasst, andere als die von mir angegebenen Quellen und Hilfsmittel nicht benutzt und die aus den benutzten Werken wörtlich oder inhaltlich entnommenen Stellen einzeln nach Ausgabe (Auflage und Jahr des Erscheinens), Band und Seite des benutzten Werkes kenntlich gemacht habe.

Ferner versichere ich, dass ich die Dissertation bisher nicht einem Fachvertreter an einer anderen Hochschule zur Überprüfung vorgelegt oder mich anderweitig um Zulassung zur Promotion beworben habe.

Ich erkläre mich einverstanden, dass meine Dissertation vom Dekanat der Medizinischen Fakultät mit einer gängigen Software zur Erkennung von Plagiaten überprüft werden kann.

Unterschrift: .....